# Flood wave characteristics and sediment transport during storm events at a channel confluence of the Anacostia River

# By Alex Bollinger

Advisor: Dr. Karen Prestegaard

April 9, 2021

**GEOL 394** 

#### Abstract

Geomorphic studies of channel confluences have focused on confluence hydraulics and consequences for channel morphology. Engineering studies have focused on confluence scour. There have been fewer studies on the variability of confluence responses and the consequences for flooding and sedimentation hazards. Additionally, geomorphic research has been primarily conducted in non-urbanized environments. Study of confluence dynamics in channelized rivers, however, could be used to evaluate the consequences of flood control measures on flow dynamics at river confluences. As urbanization and climate change continue to affect river discharges, there is a need to understand how urban rivers respond to extreme events in order to protect the communities around them. Therefore, the focus of this study is to examine flood dynamics and associated sedimentation at the confluence of the Northeast Branch and Northwest Branch Anacostia River. This study will investigate:

- a. The synchronicity of flood waves in each tributary during storm events;
- b. The threshold for transportation of bed sediment in each tributary and downstream of the river confluences; and
- c. The runoff generated in the two tributary drainage basins during storm events.

Field surveys of gravel bars were conducted in the tributaries to identify the sizes of the surface and subsurface materials. USGS measurements of the Northeast Branch and Northwest Branch were utilized in hydraulic geometry calculations. Storm hydrographs were analyzed using data collected by USGS gauges located near the confluence in each tributary. Analysis of overbank sediment deposits found along both tributaries and at the confluence showed that these deposits were made of fine sands and silts smaller than 0.25 mm. This indicated that particles of this size are held in suspension during typical river flows. Analysis of subsurface materials revealed that there is very little sand stored within the gravel beds, indicating that mobilization is frequent enough that large deposits do not build up over time. It also indicated that the gravel bars may coarsen from autumn to winter, as all of the bars were coarser during the winter. USGS data was used to calculate shear stress and the criteria for gravel bar mobilization during a storm event. Additionally, a relationship between storm intensity and the velocity of the peak flood wave was identified, which was crucial in determining the synchronicity of the storm effects between the tributaries. In total 17 storms in a 7 month period were analyzed.

No clear relationship between synchronicity of flood waves and storm characteristics were identified. All major factors analyzed in this study showed no definitive relationship to the synchronicity of an event, and all appeared to be dependent on the individual storms. This suggest that the severity of storm precipitation and their synchronicity is extremely dependent on initial conditions. This research suggests that the major influence on sediment transportation at this confluence is the number and frequency of mobilization events. The runoff response of the Northwest Branch is more rapid than the Northeast Branch. The Northeast Branch sustains longer periods of sediment deposition. Further study comparing these results to a non-urbanized system should be conducted to determine which of these behaviors is due to urbanization.

## **Background**

Rivers are one of the primary modes of transportation for sediment. River discharge, sediment supply, and bed grain size present influences sediment mobilization within the system. A rivers discharge is the volume of water passing through the system relative to a unit of time, and the momentum of this fluid is what mobilizes sediment within the system. For this study this relationship was explored in terms of storm events in an urbanized channel at a tributary junction (Figure 1). Storm events generate runoff that enters the river system leading to an increase in river discharge, which significantly increases the amount of sediment mobilized in the system.

A river confluence is where two branches join to form a single channel. The two channels meet at an angle, with gravel bars typically forming at the junction. The channel is significantly wider than the individual tributaries, as the significant increase in water volume creates a wider basin. Just downstream of the junction there is an area of scour, as the increase in flow generated by the joining of the flowing bodies transports any sediment along the river bed (Best, 1988). This exposes the underlying bedrock which will erode over time, often creating a scour hole (Best, 1988). Other of tributary junctions features include tributary mouth bars that form from bedload deposition that can change due to



Figure 1: Satellite image of the confluence of the Northwest Branch and Northeast Branch of the Anacostia River. Google Earth V 7.3.3.7786. (Jan 6, 2020). Bladensburg, MD <a href="https://earth.google.com/web">https://earth.google.com/web</a> [April 11, 2021]

the relative discharge from the tributaries (Biron, 1993). Some common sedimentation features of tributary junctions are shown below (Figure 2, Best, 1986).

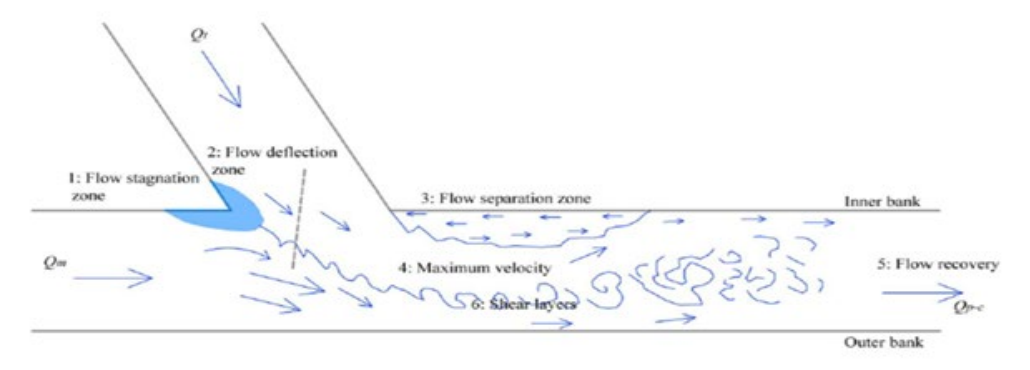


Figure 2: Illustration of fluid flow dynamics at tributary junction. From Best, 1986.

The focus of this study is the confluence of the Northeast Branch and Northwest Branch Anacostia River (see Figure 1). These tributaries are also referred to in this paper as NEB and NWB. The Northwest Branch is primarily originates in the Piedmont Province, and according to the USGS has a 127.9 km<sup>2</sup> drainage basin. The Northeast Branch is primarily originates in the Coastal Plain province, and has a 188.6 km<sup>2</sup> drainage basin with basin area ratio of 0.68, which for a non-urban stream, might correlate with the discharge ratio. The tributary junction has some non-standard features, such as the curving of the tributaries feeding into the junction. There is a bar at the mouth of the Northeast Branch, the larger of the two rivers, while there is no bar at the mouth of the Northwest Branch. The bar below the confluence is a central bar, which is not common at most tributary junctions (Best, 1988), although it is a behavior observed at other locations. Bar locations on air photos and images from 2002 to present appear stable, seeing no other major shifts in size or location during this span. The location of the bar at the mouth of the Northeast Branch suggest that discharge peaks in the Northwest Branch may frequently be higher than in the Northeast Branch, causing a backwater effect resulting in the deposition of coarse gravels. The central bar suggests that both tributaries peak synchronously, forming a central bar as both tributaries retreat from their flood stage.

Both the Northeast Branch and Northwest Branch flow through heavily urbanized areas. Due to the flooding hazard, both rivers have been channelized, with levees designed to a specification of a 100 year flood, as calculated using data from 1960 and revised in 2016. These channels were modified from their alluvial morphology to have a larger cross sectional area in the shape of a trapezoid with tall embankments of both sides of the channel. Additionally, these engineered spans of rivers are straightened. These adjustments are made in order to contain river flows, maintain flow velocities, and transport water during floods. The shape of the channel increases the cross sectional area which allows for more flow before spilling out over the embankment, with the straightening leading to an increased velocity, leading to an increase to overall discharge (USACE, 2018).

Over the past few decades, the region containing the Northeast Branch and Northwest Branch of the Anacostia River has undergone further urbanization. The construction of roads, parking lots and permanent structures replace soils with impermeable surfaces, requiring the development of large storm water management systems. This leads to a spike in the discharge of river system during large storm events. This increase in discharge generates an increase in sediment transport and prevents deposition of smaller grains in these channelized spans, leading to an increase in sediment downstream of these areas.

These bars along the Anacostia River are composed of a mixture of sands and gravels. These bars are composed of alternating layers of coarse gravels and finer sands, with gravels forming a shield layer along the surface of the gravel bar. Heterogeneous bars may contain significant quantities of sand, however the coarser grains regulate the mobility of the finer sand which underlies the surface gravels (Parker and Klingeman, 1982; Leopold, 1992). Normally, if grains had a similar density, the finer grains would mobilize more easily than the coarser grains. But in gravel bars coarser grains typically compose of the surface material, and need to be mobilized before the finer materials deposited beneath (Parker and Klingemann, 1982).

With each passing year the increase in impermeable surfaces also leads to an increase in the peak discharge during storms, as reflected by the peak annual discharge in both the NEB and NWB (Figure 3). While the distribution of peak annual flow is varied, but the maximum peak has increased over the past 50 years. While the flood prevention mechanisms are sound, they were built based on the record of the 100 year flood in 1960 (USCAE, 2018). With the increase in peak flows floods that exceed the barriers in place will become more common. On September 10<sup>th</sup>, 2020 a short duration, intense rain storm caused a rapid response on both tributaries of the Anacostia River, which overtopped its banks in several locations, leaving neighborhoods in DC, Maryland, and Virginia under several inches of water (Hermann et al., 2020). One of the affected communities was Bladensburg, Maryland, which surrounds the confluence of the Northeast and Northwest Branches. Since the original modifications to the channel were based on conditions that have significantly changed since their construction, the increasing intensity and frequency of storms has reduced the effectiveness of these flood preventions methods. While measures to mitigate flooding can be adjusted, urbanization increases the storm response in rivers. This warrants further research

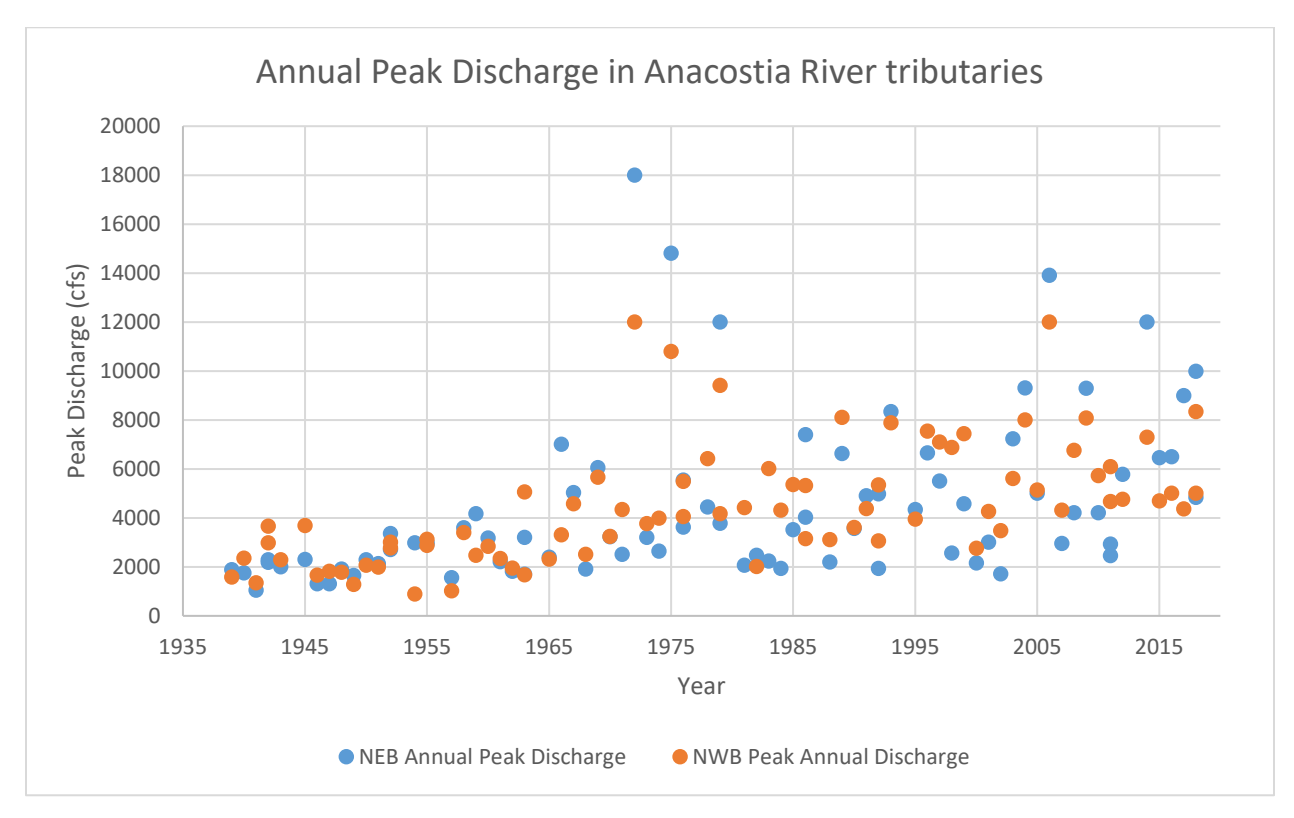


Figure 3: Annual peak discharge of the Northeast Branch and Northwest Branch. The annual peak in each branch is trending to increase every year. Data retrieved from the USGS.

Research on channel confluences and sediment transportation have typically been completed in non-urbanized channel (e.g. Best, 1988; Biron et al., 1993). This leaves a gap in understanding of how flood control channels influence sediment deposition at and below confluences, and whether changing discharge ratios from the two tributaries affect sediment erosion and deposition (Schmidt et al., 2001)

#### **Objectives and Broader Implications**

This study was conducted to generate a better understanding of sediment transport and flooding behaviors at the confluence of the Northeast and Northwest Branches of the Anacostia River. As urban areas continue to expand and climate change continues to develop, understanding the environment we are building our homes in is going to be key moving forward. This study focused on determining the timing and elevation of flood waves that arrive at the confluence of the Northwest and Northeast Branches, examine the sediment deposits that formed during flood events, and compare the runoff response from the drainage basins of the two tributaries.

Directly these three hypotheses were evaluated:

- 1. Synchronous flood waves occur during a majority of storms at the Northeast Branch-Northeast Branch confluence, with asynchronous flow being less frequent.
- 2. The runoff response (volume/basin area) of the Northwest Branch is greater than the runoff of the Northeast Branch in the majority of storms. (This may contribute to synchronicity)
- 3. Seasonal variations in storm intensity and sediment supply behaviors affects the grain composition of the gravel beds and seasons with more frequent storms deposit fine subsurface materials.

Determination of flood wave behaviors at the confluence will determine the timing of associated sediment transport events downstream of the confluence, and better evaluate flood control mechanisms. The discharge of the river downstream of the confluence is the sum of each tributary. Asynchronous flooding behavior would mean a longer duration flood event downstream of the confluence, while synchronous events have a greater peak intensity. Analysis of surface runoff contribution indicates if one of the basins contributes more to the discharge of the river system. Analyzing the grain size composition over a period of time may show that there is a seasonal relationship that plays a role in the changing channel morphology.

#### **Methods of Analysis**

Determination of Sediment Transport Criteria

Determining the composition of the surface sediments for bars along the Northwest and Northeast Branches is essential for understanding when these sediments will be mobilized. The bars of both tributaries are heterogeneous in composition, with grains varying from fine sands to coarse gravels. The surface material for beds in both tributaries is gravel. The makeup of these beds is represented in Figure 4, the surface layer of these bars functions as a shield for the finer grains that are deposited beneath the

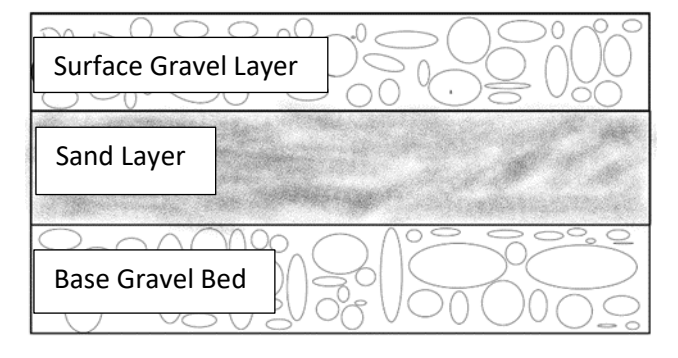


Figure 4: Illustration showing a cross section of a gravel bar. Sand layers are sandwiched between gravel layers.

gravels, and as such the bedload of a bar would not be mobilized until the surface gravels are first mobilized (Leopold, 1992). By surveying and determining the composition of the surface

material for the gravel beds in each tributary, the stress required to mobilize these grains can be determined (Wilcock et al., 2001).

Grain Size Distribution of Surface Sediments

The composition of surface sediments was determined by using the Wolman pebble count method (Wolman, 1954). The sampler paces up and down the length of the gravel bar, measuring the intermediate axis of each pebble along the path, until at least 100 pebbles are measured (Wolman, 1954). Each measured pebble is categorized by the sieve it would pass through in accordance to the ASTM standard for sieve size (ASTM, 2017). The results of the pebble counts are used to generate a cumulative mass curve, which can be used to determine the numerical distribution individual grain sizes has on the makeup of the gravel bar (Figure 5).

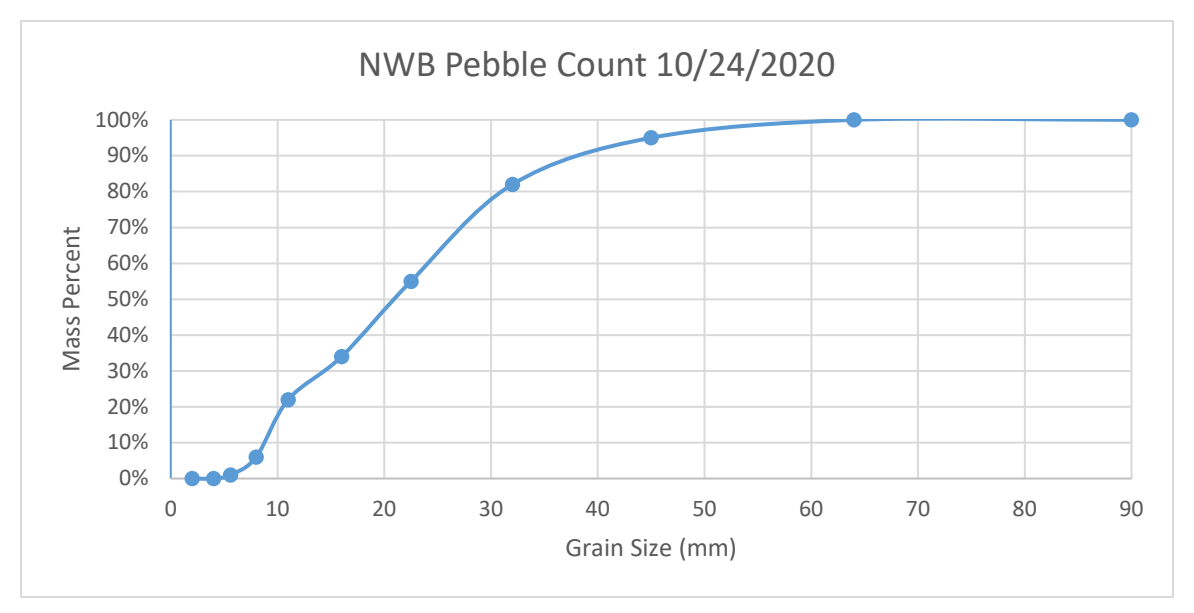


Figure 5: One of the cumulative mass curves generated from a pebble count during this study.

Relationship between stream hydraulics and gravel bar surface grain size

Prior research has investigated the criteria for the mobilization of gravel bars. The dynamics of particle mobilization is determined using the equation derived by Shields, which relates the stress exerted by the flow of a fluid with the resistance a particle exerts against movement (Shields, 1936):

$$\tau^* = \frac{\tau}{(\rho_s - \rho)gD}$$

This equation determines a unit less value known as the dimensionless shear stress ( $\tau^*$ ). In this equation,  $\tau$  is the stress exerted on the bed by a flowing water (N/m²),  $\rho_s$  is the density of sediment (kg/m³),  $\rho$  is the density of water (kg/m³), g is the acceleration of gravity (m/s²), and D is the diameter of particle which is being mobilized (m). Shields defined  $\tau^*_{crit}$  as the value of  $\tau^*$  that must be exceeded for grains to be mobilized. Shields determined that  $\tau^*_{crit} = 0.06$  from his experiments performed on flumes with homogeneous sediment sizes.

Rivers with naturally-sorted river bed sediment typically exhibit a narrow range of sediment grain sizes, but they are not homogeneous. Field data indicate that large particles in these mixtures move at  $\tau$  \* values below 0.06 and hidden finer particles move at higher  $\tau$  \* values. The stress that would mobilize the surface gravel would also mobilize the smaller sand grains, as these grains provide significantly less resistant than the larger gravels. For well-sorted gravel beds, the diameter of the 84th largest particle on the bed surface regulates mobilization of the sand layer (Leopold, 1992). The 84<sup>th</sup> largest particle is used by convention so that studies can be compared on an equal basis.

#### Assumptions used in calculations

The confluence of the Anacostia itself is not gauged, and conducting active data collection on a daily basis for the purpose of this study is impractical. The USGS however, has gauges on the tributaries a short distance upstream of the confluence (2896 meters up stream on the NEB, and 2574 meters on the NWB). No tributaries enter the channel the gauge and the junction and channelized cross section shape is constant. Therefore, in this study, USGS data (discharge, gauge height) was used to determine the hydraulics and discharge at the tributary junction. In order to use these data, the following assumptions have been made:

First, it is assumed that the channel is uniform. This requires that the width of the channel remains constant between the USGS gauge location and the tributary junction. This assumption can be tested using lidar, air photo and satellite imagery accessed through Google Earth to measure the width of the channel along the length of both the Northwest and Northeast Branches.

Second, it is assumed that at a given discharge, the flow depth is maintained along the length of the channel between the gauge and the confluence. If the width of the channel is constant, the depth of flow and flow velocity will be maintained unless backwater conditions occur ad the downstream end (e.g. high tides). This is a concern at low flow conditions, but not during high flow events (C. Hartten, pers. com., April 2<sup>nd</sup>, 2020).

Both the Northeast and Northwest Branches of the Anacostia are urban channels that have been engineered over the past half century into trapezoidal channels with little bed topography.

These channels are designed to contain and transport the rivers discharge to mitigate flooding along the entire Anacostia River. The straight channels with a uniform cross section and high embankments are designed to contain the peak flow of a 100 year flood, preventing overflow onto the flood plain (USACE, 2018).

The final assumption made is that there are no additional tributaries feeding into either the Northeast Branch or Northwest Branch between the USGS gauges and the tributary junction. This was verified using satellite imagery.

Stream geometry and hydraulics

The stress  $(\tau)$  exerted by a flowing body of water is calculated by utilizing the du Boys equation:

$$\tau = \rho dS$$

with  $\tau$  being shear stress (N/m<sup>2</sup>),  $\rho$  being the density of water (N/m<sup>3</sup>), d being average depth of water (m), and S being the energy gradient, which is the surface water gradient in uniform channels (Shields, 1936). Previous work indicates that at higher flows, the surface water

gradient is parallel to the bed gradient in uniform channels. The bed gradient was determined by using the Maryland Lidar data to determine the change in elevation between the locations of the gauging station. The distance between the gauges and the confluence were measured using satellite imagery. Together the gradient of the Northeast Branch and Northwest Branch was determined.

Given uniform channel cross sections, average boundary shear stress is primarily dependent upon average flow depth, which itself is dependent on the discharge flowing through it. This relationship can be determined from USGS measurements of discharge and channel geometry. The USGS makes field measurements of the discharge, Q, cross sectional area, A, surface stream width, W, and average velocity, V, which is reported as average velocity (Q/A). Average depth can be calculated from these measurements as A/W. Measurements from the past ten years were used to define the relationship between discharge, width, depth, and velocity. 10 years of data provides a wide range of discharge values, yet the data is recent enough that the stream morphology would be very similar to current conditions.

The relationship of discharge and critical shear stress can be determined by utilizing the USGS field measurements along with the surface grain size distribution. The determined  $D_{84}$  is used to evaluate the resisting force that surface gravels exert against motion. Using the variable depths and discharges, the critical shear stress (the maximum stress exerted upon the grains) can be calculated. For a gravel bar to be mobilized, the  $\tau^* > 0.045$  (Leopold, 1992). Using this calculated discharge threshold, USGS gauging data from August 2020 to March 2021 was used and time periods where the channel discharge exceeded the threshold were analyzed.

## Determining Flood Wave Synchronicity

In order to determine the flood waves of the tributaries arrive at the confluence, the timing of the stage and discharge peaks are compared. For the flood waves to be considered synchronous, the arrival of the peak discharge of each branch should be within 15-30 minutes of each other. This parameter was selected as 15 minutes is the data collection interval of the gauge discharge and height along the Northwest Branch, the Northeast Branch records data at 5 minute intervals. Asynchronous events are all other events where the time between discharge peaks is greater than 30 minutes.

The time elapsed between the peak floods waves passing the USGS gauges and arriving at the confluence is an important consideration. The velocity the peak flood waves is dependent on the discharge of the tributaries at a given time. Leopold and Maddock (1953) determined that the relationship between discharge and velocity in a river can be determined using power functions. Discharge and velocity data collected by the USGS was plotted, and a power trend was constructed.

The relationship for the Northwest Branch was determined to be (Figure 6a):

$$V = 0.2307Q^{0.3714}$$

The relationship for the Northeast Branch was determined to be (Figure 6b):

$$V = 0.1725Q^{0.6215}$$

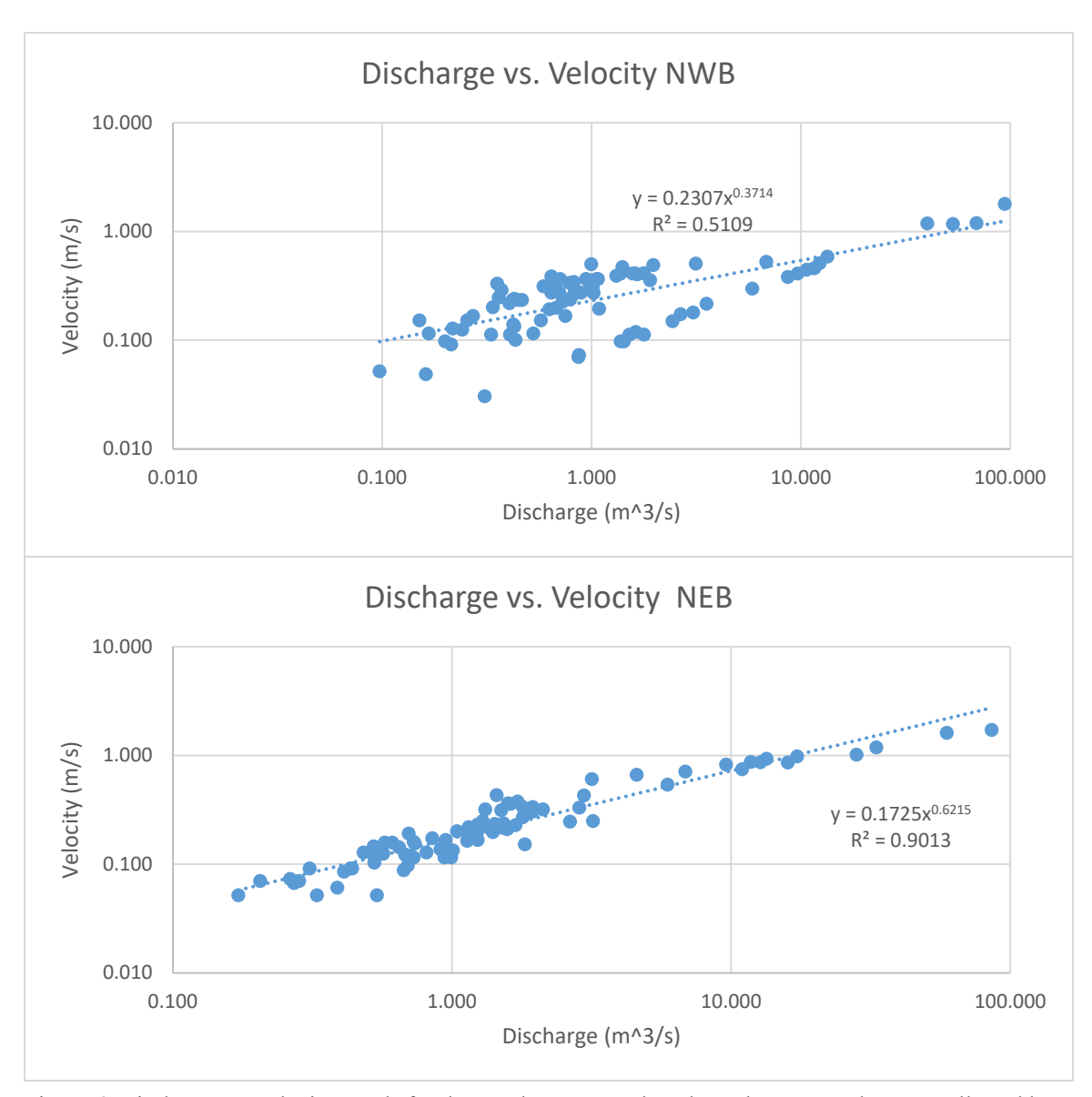


Figure 6: Discharge vs Velocity trends for the Northwest Branch and Northeast Branch. Data collected by the USGS.

The movement of the wave down the channel is different than the velocity of the fluid. In channels with uniform flow, the celerity of the flood wave tends to be faster than the average fluid velocity. To calculate the velocity of the wave the following equation can be used:

$$V_w = V_f * C$$

with  $V_w$  being the celerity of the wave (m/s),  $V_f$  being the velocity of the flow (m/s), and C is a coefficient that relates the two. In the case of a uniform rectangular channel this is determined to be 5/3 (Chow et al., 1988). The flood celerity and distance are used to evaluate the travel time to the tributary junction: Time = Distance/C.

# Runoff Calculation

The runoff of each tributary is an indication of how much water is generated in each basin. This is calculated with the equation:

$$Runoff = \frac{(Discharge * Time Interval)}{Drainage basin area}$$

This calculation returns the depth of runoff generated over the area of the drainage basin, which is expressed in millimeters. By normalizing the discharge to the basin area, the values generated in each tributary can be directly compared. The NWB is just over 30% smaller than the NEB, so this runoff value is a method to generate an apples to apples comparison of how much storm water is generated in each basin.

## Overbank & Subsurface Gravel bar Composition

The composition of the grains held in suspension and stored in the gravel bar was determined using sieve analysis of samples collected in the field. Over bank deposits are grains held in suspension during regular river flow. During floods the flow of the channel spills out over the embankment, and when the water level retreats the sediments held in suspension are deposited on the bank surface. Collecting surface samples from the banks and completing a sieve analysis of these sediments a distribution of these grain sizes can be determined. The composition of gravel bars can be determined in a similar fashion. By removing the coarser surface gravels, the finer grained sediments are able to be collected. These grains are deposited after storms as the discharge decreases, and the sediments held in suspension fall out of solution. The sands are deposited before the gravel as they have significantly less momentum than larger grains, so they are deposited on the bed first and then covered by gravels that roll along the channel base (Parker and Klingemann, 1982).

The grain size distribution was determined using a dry sieving method in accordance with ASTM D6913/D6913M-17. Samples are placed in an oven overnight to dry. The dry sample was weighed and placed in a sieve stack, which was shaken for ten minutes. The contents of each pan in the stack is weighed. These results are plotted with a cumulative curve.

#### Data analysis and error calculation

#### Surface Sediment Composition

Bars within the channelized reaches of the Northeast Branch and Northwest Branch were surveyed twice, with a period of four months elapsing between each survey. The results of the pebble counts were composited together to generate a cumulative mass curve. At the start of this study it was unclear if seasonal weather patterns directly affected the composition of gravel bars, in order to prevent bias based condition unique to the time of year. The resulting composite would better reflect the general make up of a gravel bars surface any time of year, rather than be a specific reference point. Using the composite it was determined that the regulating grain size of bed mobilization was 33 mm in the Northeast Branch and 35 mm in the Northwest Branch. The composite plots for each branch are represented by Figure 7 and Figure 8 respectively, with complete pebble count data included in the appendix.

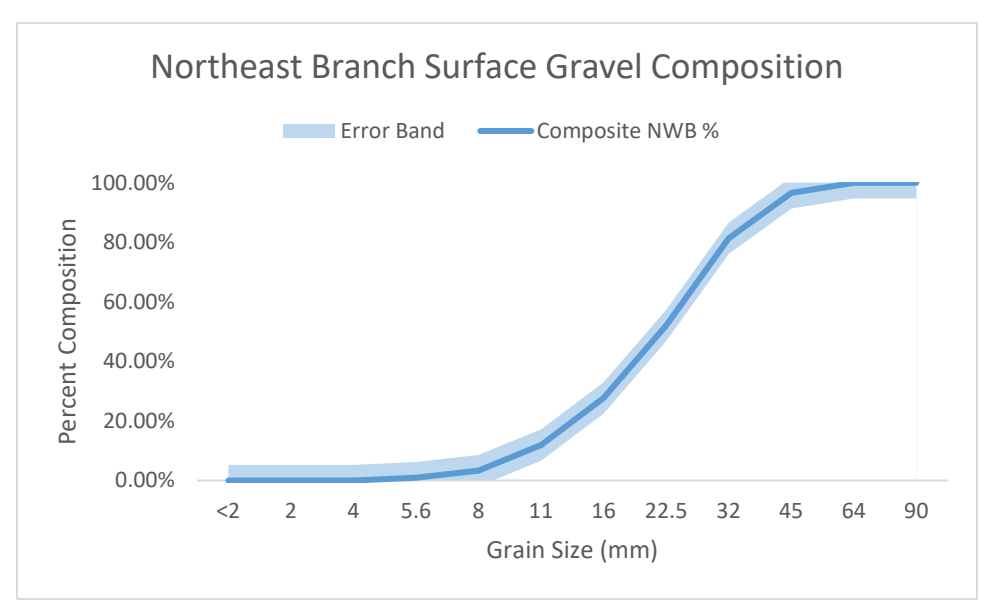


Figure 7: Plot of the composite grain size distribution of the Northeast Branch. Calculated error for surface grain size of  $\pm -5.3\%$ .

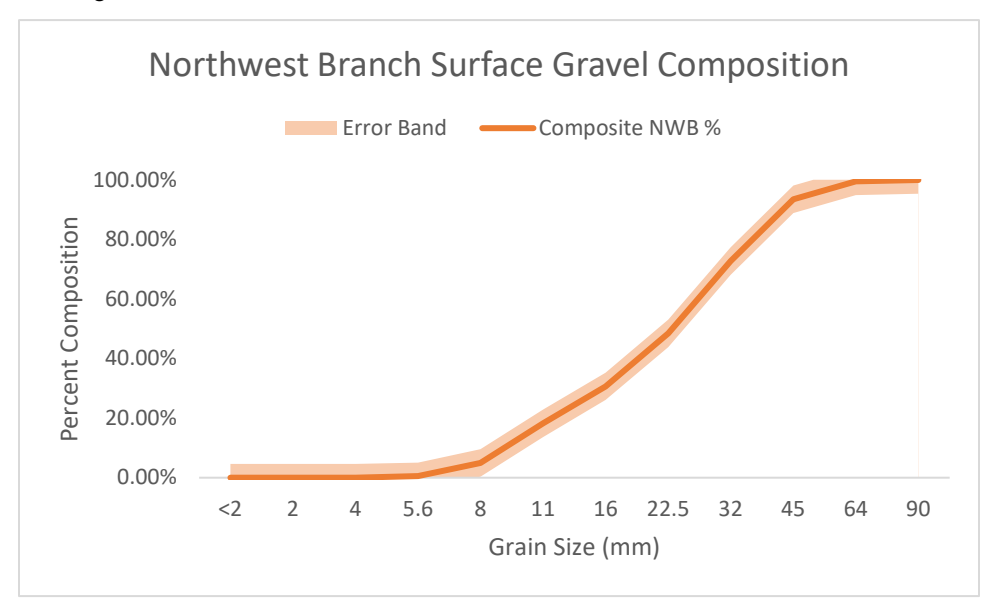


Figure 8: Plot of the composite grain size distribution of the Northwest Branch. Calculated error for surface grain size of 4.61%

The error for each distribution was calculated by taking the standard deviation of the composite pebble counts, and plotted as a field of the distribution plot. A pebble count is an efficient means of approximation, as the surveyor can rapidly determine a composition of the entire gravel bar surface. Since grains are sorted by sieve sizes rather than plotted by true diameter, there is a margin of error in terms of exact size of the regulating grain. The pebbles that are identified for the 16 mm category may be exactly 16 mm in diameter, or up to 22.4 mm. Gravel bars a fairly homogenous in size, as the physics of the flows that deposit them deposit like size grains together (Parker and Klingemann, 1982). The pebble count conducted in February 2021 resulted in a coarser distribution than the one conducted in October 2020. While an interesting result, a

more extensive survey over a longer time span is required to determine if this is a repeating pattern.

# Subsurface and Overbank Sediment Composition

Subsurface and overbank deposits were collected at the same time as pebble counts were conducted. Overbank deposits were collected from banks of each tributary, and from both sides of the channel downstream of the confluence. Subsurface samples were collected from gravel bars in each tributary and downstream of the confluence. Similar to the pebble counts, the time elapsed between analyses was to determine if there was a direct seasonal relationship in the sediments transported in the Anacostia river system.

Results from sieve analysis indicate that there may be a relationship between bed composition and seasonal weather patterns. In the Northwest Branch and downstream of the confluence there is a significant shift in composition. The February samples were noticeably coarser than the October sample, shifting from finer gravels to coarse gravel (Figure 9, Figure 10). This behavior is also seen in the Northeast Branch, but it is to a smaller degree (Figure 11).

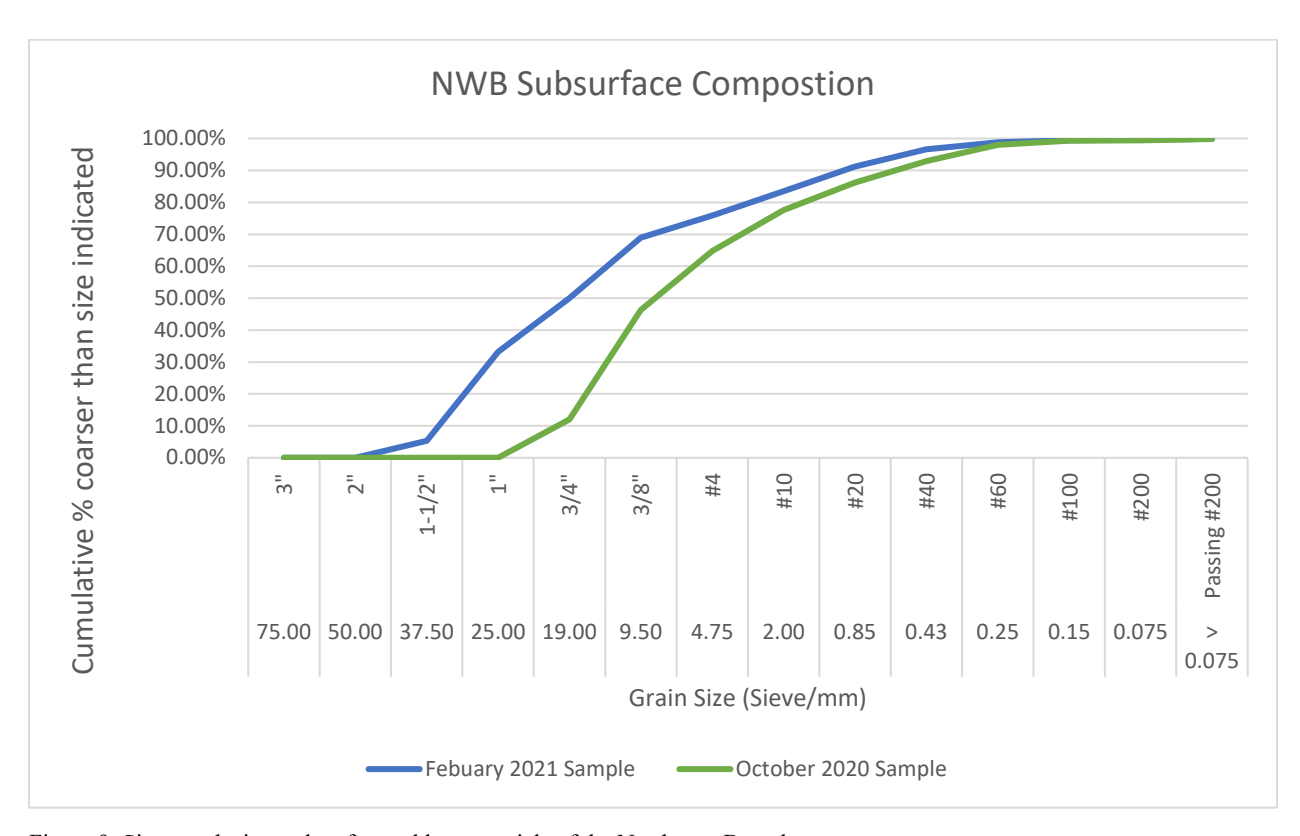


Figure 9: Sieve analysis results of gravel bar materials of the Northwest Branch.

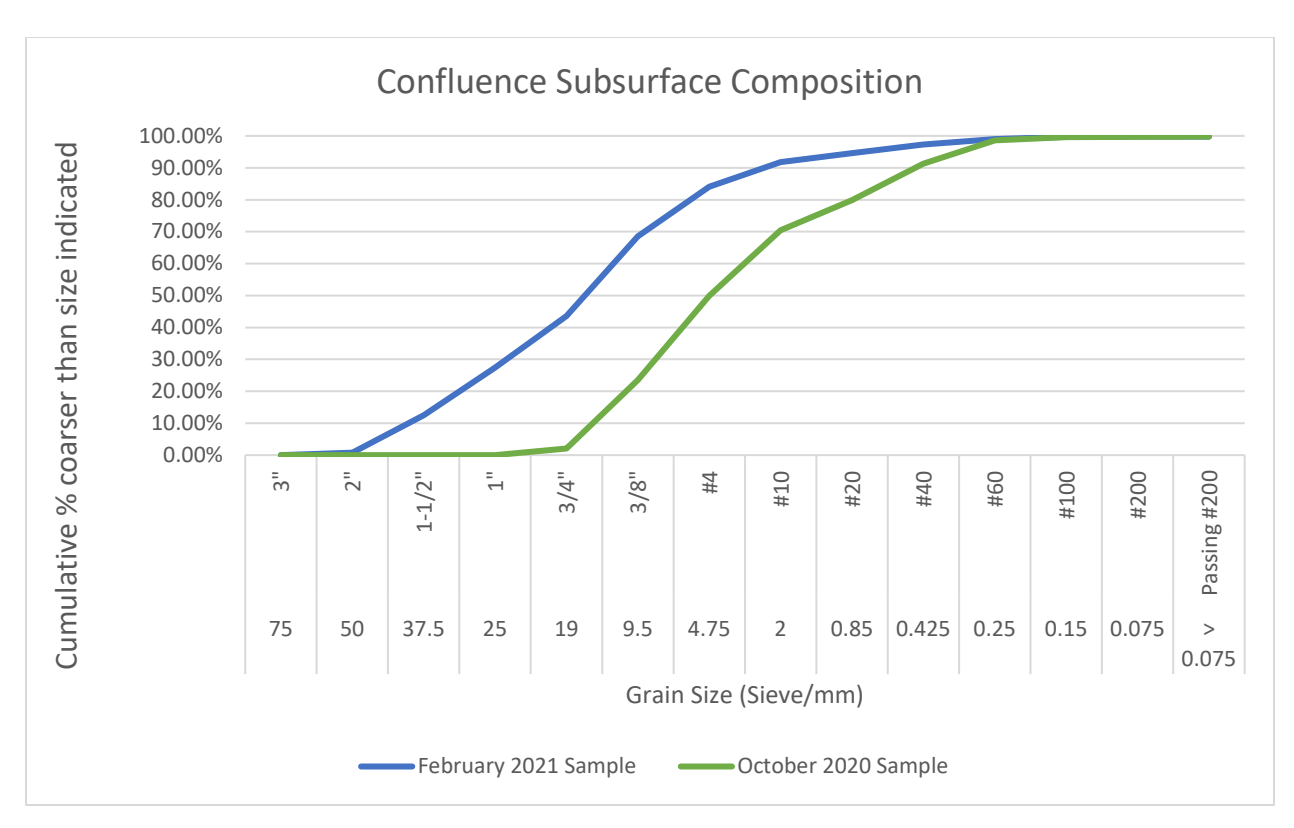


Figure 10: Sieve analysis results of subsurface material from the confluence of the NEB and NWB.

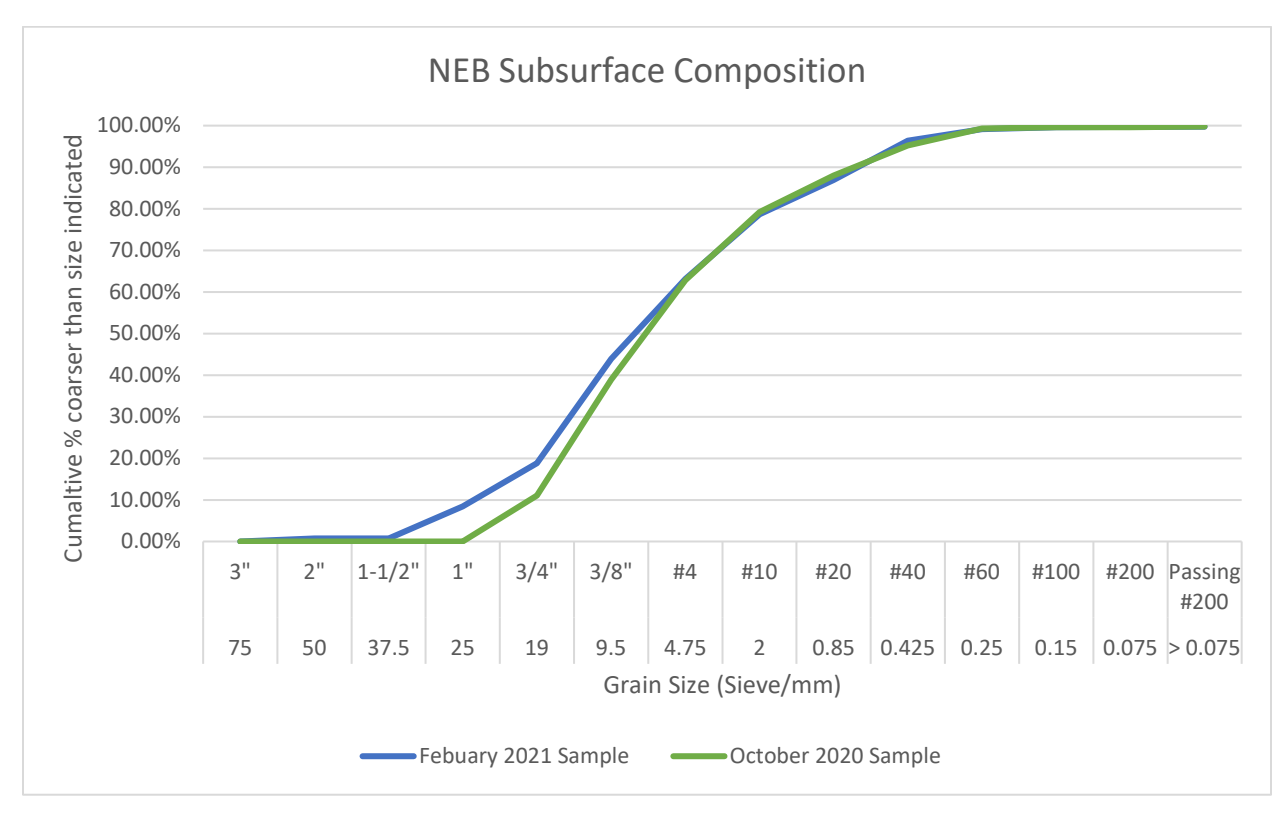


Figure 11: Sieve analysis results of gravel bar materials from the Northeast Branch.

The coarsening of the gravel bar composition may be due to the shift in weather patterns from autumn to winter. The autumn has numerous storms over a short duration, whereas winter storms are less frequent but longer in duration. Finer grains may be more likely to deposit during short duration intense storms rather than long duration, low intensity winter storms. The minor shift in the Northeast Branch also indicates that this may be caused by the limited sample size. This behavior warrants a more thorough analysis, with a monthly collection cycle over the span of 12 months.

The composition is fairly coarse, with sand sized grains composing of very little of the overall makeup of the beds. Sands are classified as grains between 2 mm to ~0.5 mm in diameter, and as the previous plots show that these only compose of less than 20% of the beds composition. Even finer grains such as silts and clays only make up small amounts of the bed composition. The overbank deposits were composed of very fine sands and silts (Figure 12). This indicates that these finer grains are likely held is suspension during regular seasonal flows, and are extremely unlikely to be deposited.

The error of sieve analysis originates from the sample lost during testing, particles can be spelled and lost while being weighted. The error is calculated by determining the yield of the analysis, and represented as a percentage of total mass lost. The results of every sieve analysis and their error is presented in the appendix.

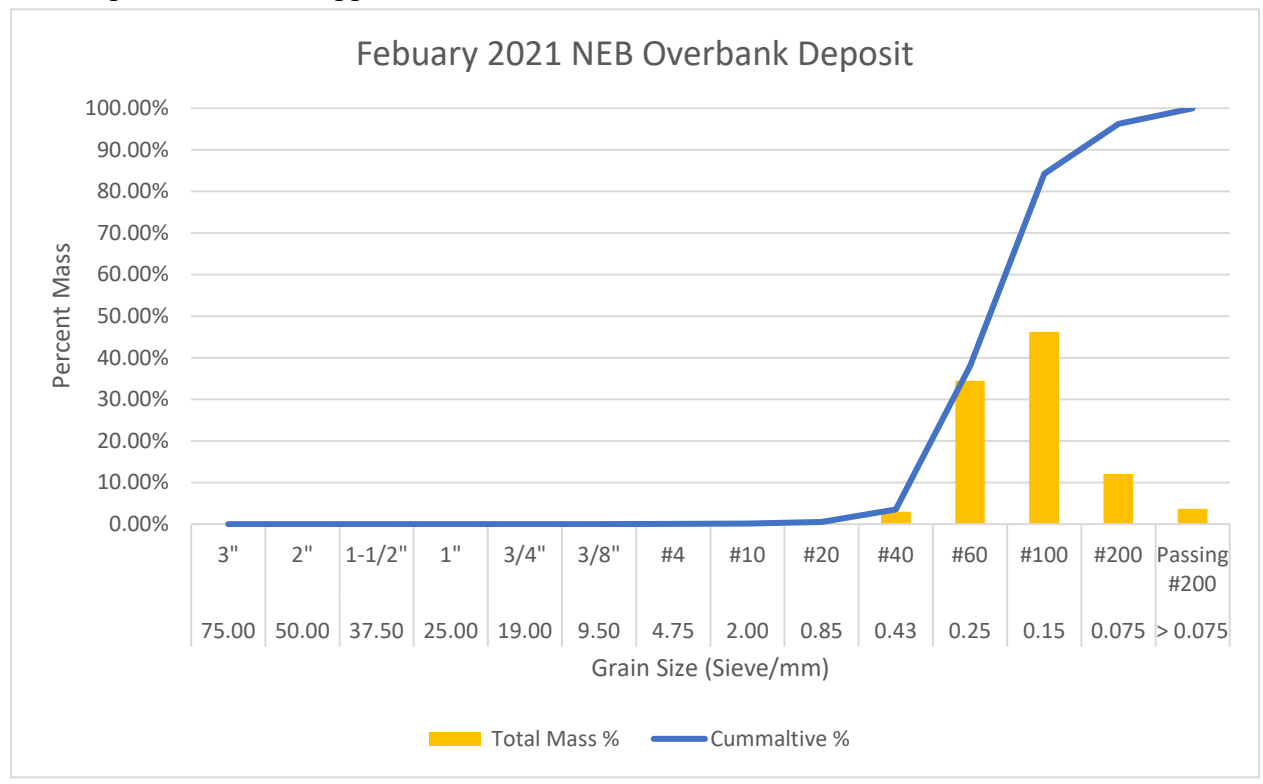
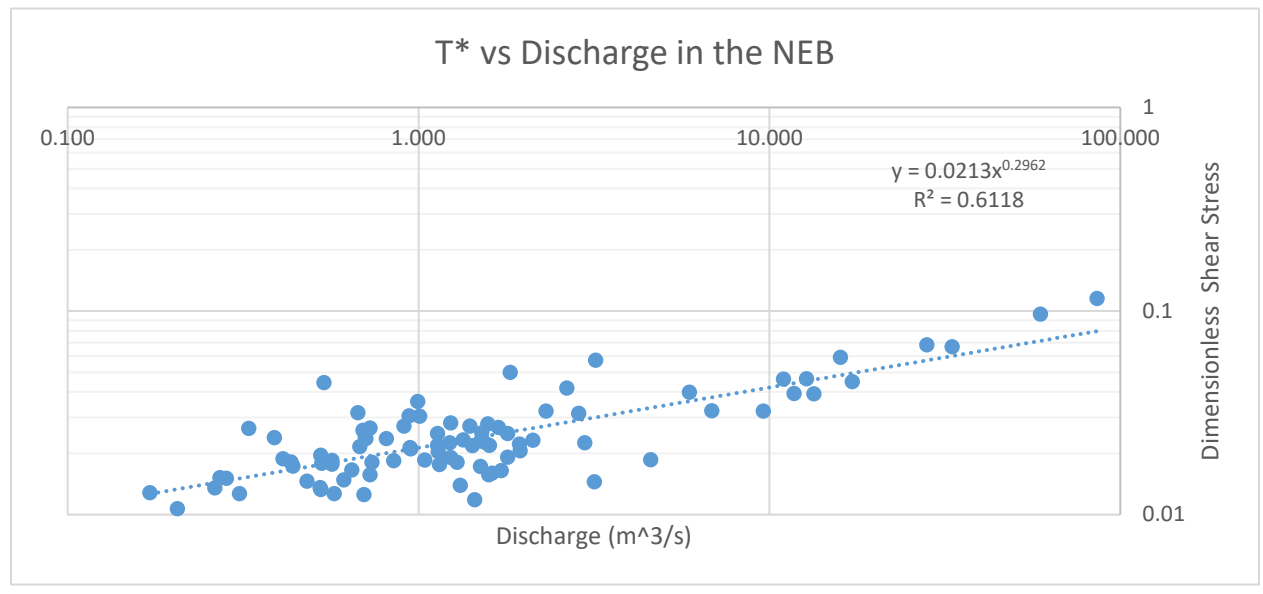


Figure 12: Sieve analysis of NEB overbank deposit collected on 2/15/2021.

## Stream Hydraulics

The stream geometry data collected by the USGS was paired with the pebble count analysis conducted in the study to generate a threshold discharge for gravel bar mobilization. The slope of the Northwest Branch was determined to be 0.0016, and the slope of the Northeast Branch was determined to be 0.0012. Google Earth pairs their imaging data with Lidar data, with a margin of error of +/- 10 cm (Wang et al., 2017). The shear stress exerted at various stages of discharge was calculated, and then plotted in order to determine a trend. A power trend was utilized, using the same method that was used to determine the relationship between discharge and velocity. The calculated threshold discharges was 12.5 m³/s in the Northeast Branch and 4.14 m³/s in the Northwest Branch (Figures 13).



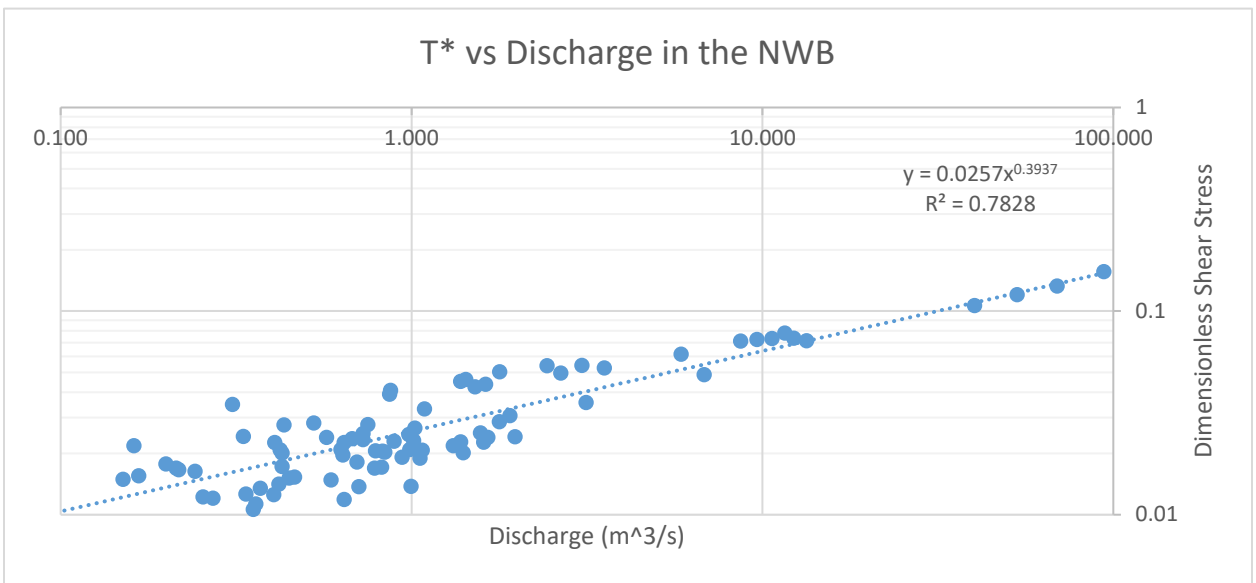


Figure 13: Plotted relationship between dimensionless shear stress and discharge in the NEB & NWB.

#### Storm analysis

A total of 17 storm events from August 2020 to February 2021 were selected and analyzed using the criteria generated from the stream geometry data and the pebble counts. Table 1 outlines the date of the event, length of the storm, peak discharges in both tributaries, as well as the timing of the events. Additionally it notes which tributary peaked first in asynchronous storms and which tributary exceeded its mobilization threshold for the longest period.

Flood wave peaks throughout a majority of the storms reached the confluence asynchronously. Of the 17 events analyzed in the study, only three events had flood wave lag times less than 15 minutes. There was no discernable relationship between lag time and the discharge of the Northeast Branch or the Northwest Branch. There also is no relationship between runoff and synchronicity, as in two of the storm events analyzed the Northeast Branch had a greater runoff response than the Northwest Branch.

One pattern identified is that the Northeast Branch will sustain the discharge required for gravel bar mobilization for a greater duration than the Northwest Branch. This trend is most likely cause by two factors, the slope of the Northwest Branch, and the greater area of the Northeast Branch drainage basin. The Northwest Branch has a steeper slope which directly increase the velocity of the flow in its channel, which in turn would increase its discharge. The Northeast Branch is around 30% large than the Northwest Branch, which translate to a larger volume of water to transport. This means the Northeast Branch drains its larger reservoir at a slower rate, which would directly cause a longer mobilization duration.

Analysis of the runoff generated during storms revealed that there is a relationship between the discharge ratio of the two branches and the runoff ratio of the two branches. Each ratio is the relationship of the peak discharge or total runoff in each branch compared to the other. A ratio of 1 indicates that the discharge or runoff of both tributaries is identical. A value greater than or less than 1 indicates one of the branches had a greater discharge peak or generated more runoff. When compared, the two ratios have a linear relationship (Figure 14). This plot shows a few

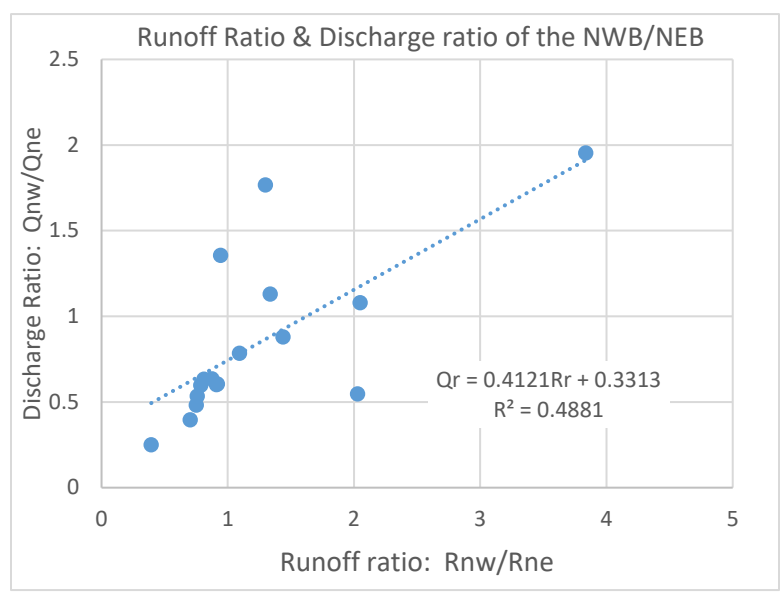


Figure 14: Runoff ratio of the NWB/NEB vs Discharge ratio of the NWB/NEB.

interesting characteristics. The runoff ratio for a majority of the storms was within a range of 0.5 to 1.5, so the amount a rainfall both basins experienced was similar in most storms. Most of the storms in this range had a discharge ratio less than 1. This suggests that Northwest Branch may be more efficient in transporting runoff. In storms where a similar amount of runoff was generated in each drainage basin, the Northwest Branch had a smaller peak discharge. When this is considered along with the observation that the Northeast Branch maintains mobilization levels

of discharge, it suggests that rainwater collected in the Northwest Branch drainage basin has a small residence time.

The runoff ratio of storms and the lag time between the peak flood waves appear to directly correlate, increasing together (Figure 15). This is most likely a result of how storm systems travel across the drainage basins. It should be expected that in storms where on basin experiences more rainfall than the other that the flood waves in that respective tributary would travel faster than the other tributary, given their velocity is directly influenced by the discharge. However, the storm event that occurred between September 10<sup>th</sup> and 11<sup>th</sup> seems to be an exception to this trend.

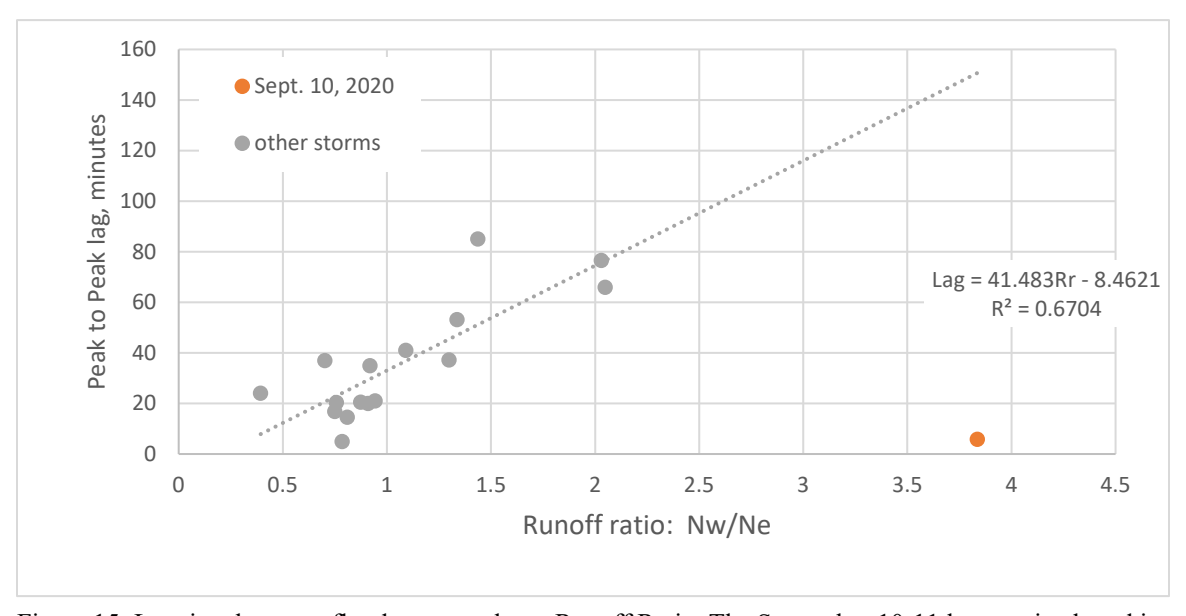


Figure 15: Lag time between flood wave peaks vs Runoff Ratio. The September 10-11th storm is plotted in orange.

 Table 1: Summary of storm events analyzed.

| Date of<br>Event       | Event Duration (hours) | Peak NWB<br>Discharge<br>(m^3/s) | Peak NEB Discharge (m^3/s) | Lag Time Between<br>Peak Flood Waves<br>(minutes) | Tributary to<br>Peak first | Tributary with the longest transportation duration | NWB Runoff<br>(mm) | NEB Runoff<br>(mm) |
|------------------------|------------------------|----------------------------------|----------------------------|---|----------------------------|--|--------------------|--------------------|
| Aug 4-5<br>2020        | 23.5                   | 213.1                            | 120.56                     | 37.2  | NWB                        | NEB  | 26.63              | 20.52              |
| Aug 6 2020             | 8.75                   | 37.64                            | 42.73                      | 85.1  | NEB                        | NWB  | 6.05               | 4.21               |
| Aug 7-8<br>2020        | 6.75                   | 21.88                            | 20.26                      | 65.9  | NEB                        | NWB  | 2.11               | 1.03               |
| Aug 12-13<br>2020      | 4.75                   | 21.88                            | 86.88                      | 24  | NEB                        | NEB  | 1.87               | 4.75               |
| Aug 16<br>2020         | 12.25                  | 23.83                            | 60                         | 37  | NWB                        | NEB  | 4.89               | 6.97               |
| Sept 3-4<br>2020       | 13.5                   | 155.93                           | 114.9                      | 21  | NWB                        | NEB  | 13.98              | 14.83              |
| Sept 10-11<br>2020     | 11.5                   | 455.63                           | 233.19                     | 5.8   | Synchronous                | Equal  | 83.73              | 21.83              |
| Oct 12<br>2020         | 4.5                    | 22.61                            | 19.98                      | 53.1  | NEB                        | NWB  | 2.26               | 1.69               |
| Oct 29-30<br>2020      | 13.5                   | 57.45                            | 90.56                      | 14.6  | Synchronous                | NEB  | 16.3               | 20.12              |
| Nov 11-12<br>2020      | 26                     | 71.32                            | 130.18                     | 76.6  | NWB                        | NEB  | 57.02              | 28.1               |
| Nov 30 -<br>Dec 1 2020 | 20.5                   | 49.81                            | 103.01                     | 16.9  | NEB                        | NEB  | 12.88              | 17.17              |
| Dec 5 2020             | 16.25                  | 28.3                             | 47.26                      | 5   | Synchronous                | NEB  | 6.78               | 8.64               |
| Dec 14-15<br>2020      | 17                     | 30.56                            | 50.66                      | 20  | NEB                        | NEB  | 8.57               | 9.42               |
| Dec 16-17<br>2020      | 21.25                  | 36.22                            | 67.64                      | 20.4  | NWB                        | NEB  | 11.13              | 14.69              |
| Dec 24-25<br>2020      | 27.75                  | 64.52                            | 82.07                      | 41  | NWB                        | NEB  | 23.52              | 21.55              |
| Jan 1-2<br>2021        | 18.5                   | 30.56                            | 50.37                      | 35  | NWB                        | NEB  | 8.56               | 9.32               |
| Feb 15-16<br>2021      | 21                     | 40.19                            | 63.11                      | 20.5  | NEB                        | NEB  | 11.43              | 13.08              |

#### Discussion

# September 10th to 11th 2020 Storm Event

Of all of the events analyzed in this study, the storm that occurred from September 10<sup>th</sup> to 11<sup>th</sup> 2020 is significant for several reasons. This was the annual peak for both the Northeast Branch and Northwest Branch, with peak discharges of 233.2 m³/s and 455.6 m³/s respectively. Second, it exhibited unique behaviors. The flood peaks arrived at the confluence synchronously, it was the only storm event where both branches had identical sediment mobilization durations, and it did not follow the increased lag time with increase runoff ratio trend. The hydrograph of this event represented in Figure 16 shows that the discharge Northwest Branch decreased rapidly after peaking, while the Northeast Branch decreased at a slower rate. The runoff ratio of this event was a 3.8 and the discharge ratio was 1.95, both the highest of the events analyzed. This comparisons of ratios is interesting, as is shows that the Northwest Branch more rapidly transported the rainwater that collected in its drainage basin. This is a strong indicator that the Northwest Branch rapidly moves runoff.

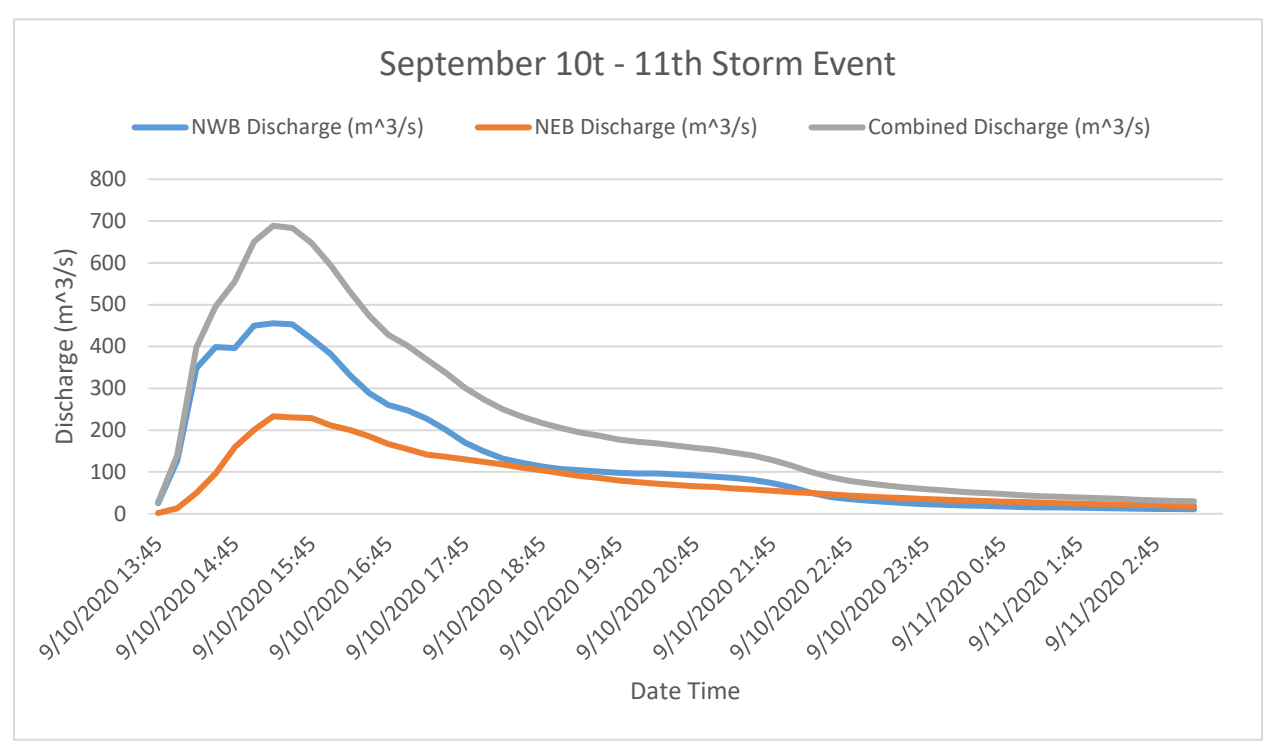


Figure 16: Storm Event Hydrograph from September 10th to 11th 2020.

#### Flood Wave Synchronicity

There is a clear that the velocity of flood waves traveling down river is strongly related to the intensity of storm events. The relationships that were identified between runoff ratios, discharge ratios, and lag time indicate that there is an inherent relationship between storm event intensity and the arrival times of flood wave, it just was not the relationship anticipated. Instead of the intensity of the storm events determining synchronicity, it is most likely how similarly intense the storm is in each drainage basin. Storm events with runoff ratios close to 1 generally had smaller lag times than events with greater runoff ratios (Figure 15). Overall, the lag time between

peak flood waves was short. The average lag time between the flood wave peaks was 34 minutes, which would still result in a significant influx of water arriving at the confluence in a short time span.

#### Area for future research on Synchronicity

The choice to define events with a lag time less than 15 minutes was selected because of the data collection cycle of USGS gages. An investigation into the hydraulics directly at the confluence during storm events may generate a better distinction between synchronous and asynchronous. Storm data at a urban confluence and a rural confluence can also be compared to see how river systems in different environments would react to similar storms. Additionally, a study of where storm events are most intense may yield insight on how lag time between flood waves is influenced by the path that storms travel. Using radar data, it would be possible to track the path storms take over the drainage basins. Pairing this with hydrographs during this period of time could explain the flood response the tributaries exhibit during individual storms.

# Runoff response and interval of sediment transportation

The runoff response during storm events was similar in both tributaries, with most storms having a runoff ratio between 0.5-1.5. The discharge ratio's indicates that the Northwest Branch has a more rapid runoff response, transporting the runoff generated in its drainage with greater efficiency. The Northeast Branch has a longer residence time for runoff, leading to longer periods of sediment mobilization. The rate that the Northwest Branch drains it basin shows that it has a very rapid runoff response during storm, with a shorter duration for sediment transportation. This suggest that the sediment downstream of confluence would consist mostly of materials from the Northeast Branch.

# Area for future research on runoff response and sediment transportation

The unique runoff response of the September 10<sup>th</sup>-11<sup>th</sup>, 2020 storm event warrants a investigation into other annual peak storm events. Was the high discharge ratios and runoff ratios unique, or is there a threshold which when exceeded the same behavior repeats? The USGS has extensive records of both the Northeast Branch and Northwest Branch, allowing an extensive investigation into the history of flooding at this confluence. It could also provide insight on how urbanization over time has affected flood response in the system. Using historical records, it could be determined if the Northwest Branch has always rapidly dispersed runoff, or if human activity has changed its behavior.

#### Seasonal storm behavior and gravel bar composition

The data in this study suggest that for sediment mobilization in urban confluences it may not be the characteristic of a storm that effect gravel bed mobilization, but the quantity of storms. When beginning this study it was expected that over a period of 12 months there may have been 10 events to analyze. Instead there were 17 over a span of only 7 months. The subsurface sediment data also shows that there is very little fine materials stored upstream of the confluence or deposited immediately downstream of it. This gives a strong indication that these mobilizing storms are so frequent that sand deposits are mobilized to quickly to build up. The subsurface composition did coarsen between October and February, indicating that seasonal weather may have affect the size of grains deposited. The storms analyzed from August 2020 through October 2020 typically had a duration of 12 hours or less. Storms analyzed from November 2020 to

February 2021 all had a duration between 16 to 28 hours. The extend duration of the winter storms could keep fine grain sediments in suspension for extended periods of time and causing the shift in composition.

Area for future research of seasonal storm behavior and gravel bar composition

Work conducted on gravel beds in Ontario, Canada also found that urbanization has led to an increase in sediment mobilization events (Plumb et al., 2017). This study did not find shifts in composition due to a shift in seasonal weather patterns. A longer duration study should be conducted over the span of several years, analyzing subsurface materials to determine if the shift in grain composition is replicated. This same study should also be conducted at a non-urbanized confluence to see determine if seasonal shifts in grain size composition is unique to regions where sediment mobilization events are frequent.

#### Conclusion

Urbanization and engineered channels have a clear impact on the sediment transport regime of a river system. Data analyzed shows that flood waves at the confluence of the Northeast Branch and Northwest Branch of the Anacostia typically arrive asynchronously during storm events, disproving that synchronous behavior was the norm. Of the 17 storms analyzed only 3 exhibited synchronous flood wave behavior. The runoff response of the Northwest Branch is similar in magnitude for most storm events and more rapidly drains its basin, supporting that the Northwest Branch runoff response if greater than the Northeast Branch during storm events. The runoff generated during storm events is similar in both branches, but the Northwest Branch dissipates the generated water through its system more efficiently. This results in rapid sediment mobilization. This runoff response did not play a factor in synchronicity, and the two properties were determined to be independent from one another. The sediment analysis indicated that fine grain particles don't settle in the reaches examined during this study. It is a strong possibility that the number of storms that mobilize gravel bars plays a major role in the transportation of fine sediments downstream. Additional analysis of urbanized systems should be conducted with a stronger focus on the residence times of sediments, and the implications that has on downstream sediment build up. Analysis of subsurface materials supports the hypothesis that seasonal weather patterns may contribute to a change in gravel bar composition. Analysis shows that subsurface materials in both tributaries coarsened in composition between the autumn and winter. This behavior indicates that long duration winter storms keep fine grained sediment in suspension, and prevent deposition along the beds of the river system. Urbanization is causing a change to the geomorphology of the rivers in our environment. The number of storms which mobilize gravel bars and subsurface materials is increase as our cities and towns grow. This study serves as an initial investigation of urbanized river systems, but more studies comparing urban system with non-urban systems to determine which behaviors identified by this research are cause by urbanization.

# **Bibliography**

ASTM D6913 / D6913M-17, Standard Test Methods for Particle-Size Distribution (Gradation) of Soils Using Sieve Analysis, ASTM International, West Conshohocken, PA, 2017, www.astm.org

Best, J. (1988). Sediment transport and ben morphology at river channel confluences. *Sedimentology*, *35*, 481-498.

Biron, P., Roy, A., Best, J., Boyer, C. (1993). Bed morphology and sedimentology at the confluence of unequal depth channels, *Geomorphology*, 8, 115-129.

Chow, V. T., Maidment, D. R., and Mays, L.W. (1988), *Applied Hydrology*, McGraw-Hill, New York.

Hermann, P. Samenow, J. Moyer, J. (September, 10<sup>th</sup>, 2020). Record-setting rain deluges Washington, submerging roads and stranding drivers. *Washington Post*. <a href="https://www.washingtonpost.com/local/washington-dc-flooding/2020/09/10/e9d50aec-f396-11ea-999c-67ff7bf6a9d2\_story.html">https://www.washingtonpost.com/local/washington-dc-flooding/2020/09/10/e9d50aec-f396-11ea-999c-67ff7bf6a9d2\_story.html</a>

Schmidt, J.C., Parnell, R.A., Grams, R.E., Hazel, J.E., Kaplinkski, M.A., Stevens, L.E., Hoffnagle, T.L. (2001). *The 1996 Controlled flood in Grand Canyon: Flow, Sediment Transport, and Geomorphic change, 11(3),* 657-671.

Shields, A. (1936). Anwendung der Aehnlichkeitsmechanik und der Turbulenzforschungauf die Geschiebebewegung, *Mitteilungender PreussischenVersuchsanstalt fur Wasserbau und Schiffbau* (Translated to English by W. P. Ott and J. C. van Uchelen, Calif., Inst. of Technol., Pasadena, 1936.)

Leopold, L.B. (1992). Sediment Size that Determines Channel Morphology. In Billi, P. Hey, R.D., Thorne, C.R., Tacconi, P., *Dynamics of Gravel-bed Rivers*. John Wiley & Sons Ltd.

Leopold, L.B., Maddock, T. (1953). *The Hydraulic Geometry of Stream Channels and Some Physiographic Implications*. USGS Professional Paper 252. Report prepared for the United States Geological Survey. Retrieved on October 31<sup>st</sup>, 2020, from <a href="https://pubs.usgs.gov/pp/0252/report.pdf">https://pubs.usgs.gov/pp/0252/report.pdf</a>

Nelson, P., Smith, J., & Miller, J. (2006) Evolution of channel morphology and hydrologic response in an urbanized drainage basin. *Earth Surface Processes and Landforms*. 31, 1063 - 1079.

Parker, G., Klingeman, P.C., 1982. On Why Gravel Bed Streams Are Paved. *Water Resources Research* 18(5): 1409-1423

Plumb, B. D., Annable, W. K., Thompson, P. J., & Hassan, M. A. (2017). The impact of urbanization on temporal changes in sediment transport in a gravel bed channel in Southern Ontario, Canada. *Water Resources Research*, 53, 8443–8458. <a href="https://doi.org/10.1002/2016WR020288">https://doi.org/10.1002/2016WR020288</a>

United States. Army. Corps of Engineers (USACE). (2018) Anacostia Watershed Restoration, Prince George's County, Maryland Ecosystem Restoration Feasibility Study and Integrated Environmental Assessment. Retrieved October 31st, 2020, from <a href="https://www.nab.usace.army.mil/Portals/63/docs/Environmental/Anacostia/AWR\_PG\_Main\_Report\_FINAL\_Dec2018.pdf">https://www.nab.usace.army.mil/Portals/63/docs/Environmental/Anacostia/AWR\_PG\_Main\_Report\_FINAL\_Dec2018.pdf</a>

Wang, Yinsong & Zou, Yajie & Henrickson, Kristian & Tang, Jinjun & Park, byung-jung. (2017). Google Earth elevation data extraction and accuracy assessment for transportation applications. *PLoS ONE*. 12. 10.1371/journal.pone.0175756.

Wilcock, P.R., Kenworthy, S.T., Crowe, J.C., 2001, Experimental study of the transport of mixed sand and gravel. *Water Resources Research* 37(12): 3349-3358

Wolman, M. G., 1954, A Method of Sampling Coarse River-Bed Material. *Transactions, American Geophysical Union* 35(6): 951-956

# Appendix

| Northwest Branch  | stream hyd   | lraulic/criti | cal shear str | ess       |                |                      |       |
|-------------------|--------------|---------------|---------------|-----------|----------------|----------------------|-------|
| Date Calculations | Q<br>(m^3/s) | Width (m)     | Area (m^2)    | Depth (m) | Velocity (m/s) | Shear Stress (N/m^2) | T*    |
| 2/2/2010 9:26     | 0.98         | 10.21         | 2.79          | 0.27      | 0.35           | 14.06                | 0.026 |
| 3/31/2010 10:17   | 1.65         | 15.54         | 4.10          | 0.26      | 0.40           | 13.58                | 0.025 |
| 5/11/2010 9:36    | 0.64         | 9.45          | 2.35          | 0.25      | 0.27           | 12.82                | 0.024 |
| 6/29/2010 8:35    | 1.61         | 15.48         | 3.87          | 0.25      | 0.41           | 12.89                | 0.024 |
| 7/8/2010 8:11     | 0.24         | 10.82         | 1.94          | 0.18      | 0.12           | 9.24                 | 0.017 |
| 8/26/2010 11:08   | 0.43         | 9.45          | 1.79          | 0.19      | 0.24           | 9.78                 | 0.018 |
| 10/13/2010 9:03   | 0.41         | 14.63         | 3.64          | 0.25      | 0.11           | 12.82                | 0.024 |
| 12/9/2010 10:43   | 0.43         | 14.02         | 4.26          | 0.30      | 0.10           | 15.67                | 0.029 |
| 2/9/2011 10:30    | 1.09         | 15.24         | 5.55          | 0.36      | 0.20           | 18.75                | 0.035 |
| 3/11/2011 10:46   | 6.82         | 24.08         | 12.91         | 0.54      | 0.53           | 27.63                | 0.052 |
| 4/14/2011 9:33    | 1.91         | 15.85         | 5.35          | 0.34      | 0.36           | 17.39                | 0.033 |
| 5/27/2011 8:35    | 0.53         | 14.63         | 4.53          | 0.31      | 0.12           | 15.96                | 0.030 |
| 7/25/2011 8:22    | 0.16         | 13.72         | 3.29          | 0.24      | 0.05           | 12.35                | 0.023 |
| 10/6/2011 8:48    | 0.57         | 14.17         | 3.74          | 0.26      | 0.15           | 13.61                | 0.025 |
| 12/20/2011 9:13   | 0.79         | 14.63         | 3.32          | 0.23      | 0.24           | 11.68                | 0.022 |
| 2/8/2012 10:04    | 0.75         | 14.63         | 4.46          | 0.30      | 0.17           | 15.70                | 0.029 |
| 4/9/2012 9:30     | 0.63         | 14.33         | 3.29          | 0.23      | 0.19           | 11.83                | 0.022 |
| 6/14/2012 8:40    | 0.43         | 14.33         | 3.17          | 0.22      | 0.13           | 11.39                | 0.021 |
| 8/3/2012 8:47     | 0.21         | 12.65         | 2.36          | 0.19      | 0.09           | 9.61                 | 0.018 |
| 9/17/2012 12:00   | 0.10         | 11.58         | 1.85          | 0.16      | 0.05           | 8.22                 | 0.015 |
| 10/9/2012 10:16   | 0.42         | 13.23         | 3.03          | 0.23      | 0.14           | 11.79                | 0.022 |
| 12/3/2012 13:00   | 0.40         | 13.38         | 1.85          | 0.14      | 0.22           | 7.12                 | 0.013 |
| 2/11/2013 13:16   | 3.14         | 15.94         | 6.23          | 0.39      | 0.51           | 20.15                | 0.038 |
| 4/16/2013 12:22   | 0.64         | 9.14          | 1.98          | 0.22      | 0.32           | 11.15                | 0.021 |
| 6/10/2013 13:01   | 5.86         | 29.32         | 19.79         | 0.67      | 0.30           | 34.77                | 0.065 |
| 6/11/2013 8:57    | 11.58        | 29.47         | 25.27         | 0.86      | 0.46           | 44.17                | 0.083 |
| 6/20/2013 11:19   | 0.68         | 13.23         | 3.44          | 0.26      | 0.20           | 13.39                | 0.025 |
| 8/21/2013 10:49   | 0.20         | 10.36         | 2.03          | 0.20      | 0.10           | 10.07                | 0.019 |
| 10/31/2013 12:27  | 0.31         | 26.70         | 10.22         | 0.38      | 0.03           | 19.72                | 0.037 |
| 12/11/2013 14:19  | 1.63         | 28.19         | 13.56         | 0.48      | 0.12           | 24.78                | 0.046 |
| 3/5/2014 10:47    | 1.52         | 28.80         | 13.47         | 0.47      | 0.11           | 24.09                | 0.045 |
| 4/23/2014 10:44   | 1.38         | 28.59         | 14.21         | 0.50      | 0.10           | 25.61                | 0.048 |
| 6/17/2014 12:45   | 0.84         | 13.20         | 2.95          | 0.22      | 0.29           | 11.50                | 0.022 |
| 8/19/2014 12:28   | 0.42         | 11.58         | 1.80          | 0.16      | 0.23           | 8.02                 | 0.015 |
| 10/17/2014 13:18  | 0.87         | 28.50         | 12.26         | 0.43      | 0.07           | 22.17                | 0.041 |
| 12/2/2014 13:17   | 3.54         | 28.25         | 16.35         | 0.58      | 0.22           | 29.81                | 0.056 |
| 2/4/2015 13:26    | 1.02         | 12.89         | 3.77          | 0.29      | 0.27           | 15.07                | 0.028 |

Supplemental 1: Stream geometry data for the Northwest Branch (February 2010- February 2015)

| Date             | Q       | Width | Area  | Depth | Velocity | Shear Stress | T*    |
|------------------|---------|-------|-------|-------|----------|--------------|-------|
|                  | (m^3/s) | (m)   | (m^2) | (m)   | (m/s)    | (N/m^2)      |       |
| 4/14/2015 14:32  | 2.66    | 28.04 | 15.33 | 0.55  | 0.17     | 28.16        | 0.053 |
| 6/10/2015 11:49  | 1.00    | 13.11 | 1.99  | 0.15  | 0.50     | 7.81         | 0.015 |
| 8/6/2015 13:12   | 0.37    | 8.66  | 1.28  | 0.15  | 0.29     | 7.63         | 0.014 |
| 9/24/2015 14:30  | 0.15    | 6.07  | 0.99  | 0.16  | 0.15     | 8.44         | 0.016 |
| 10/7/2015 12:27  | 0.35    | 9.14  | 1.07  | 0.12  | 0.33     | 6.02         | 0.011 |
| 11/30/2015 9:48  | 0.64    | 12.65 | 1.65  | 0.13  | 0.39     | 6.74         | 0.013 |
| 12/1/2015 14:33  | 9.66    | 29.44 | 23.50 | 0.80  | 0.41     | 41.13        | 0.077 |
| 2/10/2016 13:12  | 1.43    | 28.53 | 14.49 | 0.51  | 0.10     | 26.17        | 0.049 |
| 4/8/2016 10:23   | 2.43    | 27.22 | 16.17 | 0.59  | 0.15     | 30.60        | 0.057 |
| 6/8/2016 10:10   | 0.71    | 12.80 | 1.93  | 0.15  | 0.37     | 7.78         | 0.015 |
| 7/19/2016 9:47   | 0.94    | 12.19 | 2.57  | 0.21  | 0.37     | 10.87        | 0.020 |
| 9/27/2016 13:05  | 0.87    | 26.30 | 11.80 | 0.45  | 0.07     | 23.11        | 0.043 |
| 9/29/2016 13:19  | 10.65   | 29.75 | 23.97 | 0.81  | 0.45     | 41.51        | 0.078 |
| 10/6/2016 13:49  | 0.45    | 11.43 | 1.90  | 0.17  | 0.23     | 8.58         | 0.016 |
| 12/7/2016 10:48  | 3.06    | 28.53 | 17.00 | 0.60  | 0.18     | 30.70        | 0.057 |
| 2/6/2017 13:29   | 0.36    | 11.80 | 1.47  | 0.12  | 0.25     | 6.41         | 0.012 |
| 4/11/2017 12:14  | 0.70    | 12.68 | 2.53  | 0.20  | 0.28     | 10.27        | 0.019 |
| 6/21/2017 13:13  | 0.46    | 11.73 | 1.98  | 0.17  | 0.23     | 8.69         | 0.016 |
| 7/28/2017 16:57  | 53.24   | 34.14 | 45.24 | 1.33  | 1.17     | 68.28        | 0.128 |
| 7/28/2017 17:20  | 69.09   | 39.62 | 57.88 | 1.46  | 1.19     | 75.25        | 0.141 |
| 8/8/2017 10:14   | 1.78    | 28.90 | 15.98 | 0.55  | 0.11     | 28.49        | 0.053 |
| 9/28/2017 16:25  | 0.27    | 12.34 | 1.64  | 0.13  | 0.17     | 6.82         | 0.013 |
| 9/28/2017 16:27  | 0.25    | 12.34 | 1.66  | 0.13  | 0.15     | 6.94         | 0.013 |
| 10/18/2017 13:45 | 0.33    | 10.97 | 2.93  | 0.27  | 0.11     | 13.74        | 0.026 |
| 12/14/2017 13:52 | 0.34    | 12.04 | 1.67  | 0.14  | 0.20     | 7.16         | 0.013 |
| 2/21/2018 13:14  | 0.82    | 12.68 | 2.39  | 0.19  | 0.34     | 9.70         | 0.018 |
| 2/26/2018 11:07  | 1.40    | 13.47 | 2.98  | 0.22  | 0.47     | 11.40        | 0.021 |
| 4/18/2018 11:49  | 1.31    | 14.02 | 3.36  | 0.24  | 0.39     | 12.36        | 0.023 |
| 4/27/2018 10:13  | 12.29   | 29.87 | 24.15 | 0.81  | 0.51     | 41.66        | 0.078 |
| 6/19/2018 12:24  | 0.59    | 11.52 | 1.88  | 0.16  | 0.31     | 8.39         | 0.016 |
| 7/23/2018 9:39   | 13.37   | 28.90 | 22.76 | 0.79  | 0.59     | 40.58        | 0.076 |
| 8/24/2018 10:21  | 0.78    | 12.41 | 2.31  | 0.19  | 0.34     | 9.61         | 0.018 |
| 10/9/2018 13:18  | 1.07    | 12.80 | 2.92  | 0.23  | 0.37     | 11.74        | 0.022 |
| 11/6/2018 12:14  | 40.21   | 28.86 | 33.82 | 1.17  | 1.19     | 60.36        | 0.113 |
| 12/6/2018 14:27  | 1.38    | 13.35 | 3.34  | 0.25  | 0.41     | 12.91        | 0.024 |
| 2/4/2019 11:10   | 1.57    | 13.75 | 3.82  | 0.28  | 0.41     | 14.31        | 0.027 |
| 4/24/2019 10:51  | 1.06    | 13.84 | 2.89  | 0.21  | 0.37     | 10.76        | 0.020 |
| 6/19/2019 12:49  | 1.97    | 15.12 | 4.01  | 0.27  | 0.49     | 13.68        | 0.026 |
| 8/22/2019 12:18  | 1.78    | 13.62 | 4.29  | 0.32  | 0.41     | 16.23        | 0.030 |
| 9/18/2019 13:12  | 0.22    | 9.14  | 1.67  | 0.18  | 0.13     | 9.42         | 0.018 |
| 10/8/2019 12:13  | 0.17    | 8.47  | 1.45  | 0.17  | 0.12     | 8.81         | 0.016 |
| 12/19/2019 12:50 | 0.89    | 12.83 | 3.24  | 0.25  | 0.27     | 13.02        | 0.024 |
| 2/11/2020 11:11  | 8.66    | 28.93 | 22.67 | 0.78  | 0.38     | 40.37        | 0.076 |
| 3/27/2020 10:18  | 1.01    | 13.17 | 3.34  | 0.25  | 0.30     | 13.09        | 0.024 |
| 5/28/2020 10:24  | 0.83    | 13.62 | 3.08  | 0.23  | 0.27     | 11.63        | 0.022 |
| 8/10/2020 12:24  | 0.99    | 13.44 | 3.09  | 0.23  | 0.32     | 11.86        | 0.022 |
| 9/10/2020 19:53  | 94.01   | 30.48 | 52.49 | 1.72  | 1.79     | 88.72        | 0.166 |
| 9/17/2020 10:04  | 0.73    | 10.88 | 3.00  | 0.28  | 0.24     | 14.21        | 0.027 |
| 10/2/2020 12:20  | 0.73    | 12.50 | 3.21  | 0.26  | 0.23     | 13.25        | 0.025 |

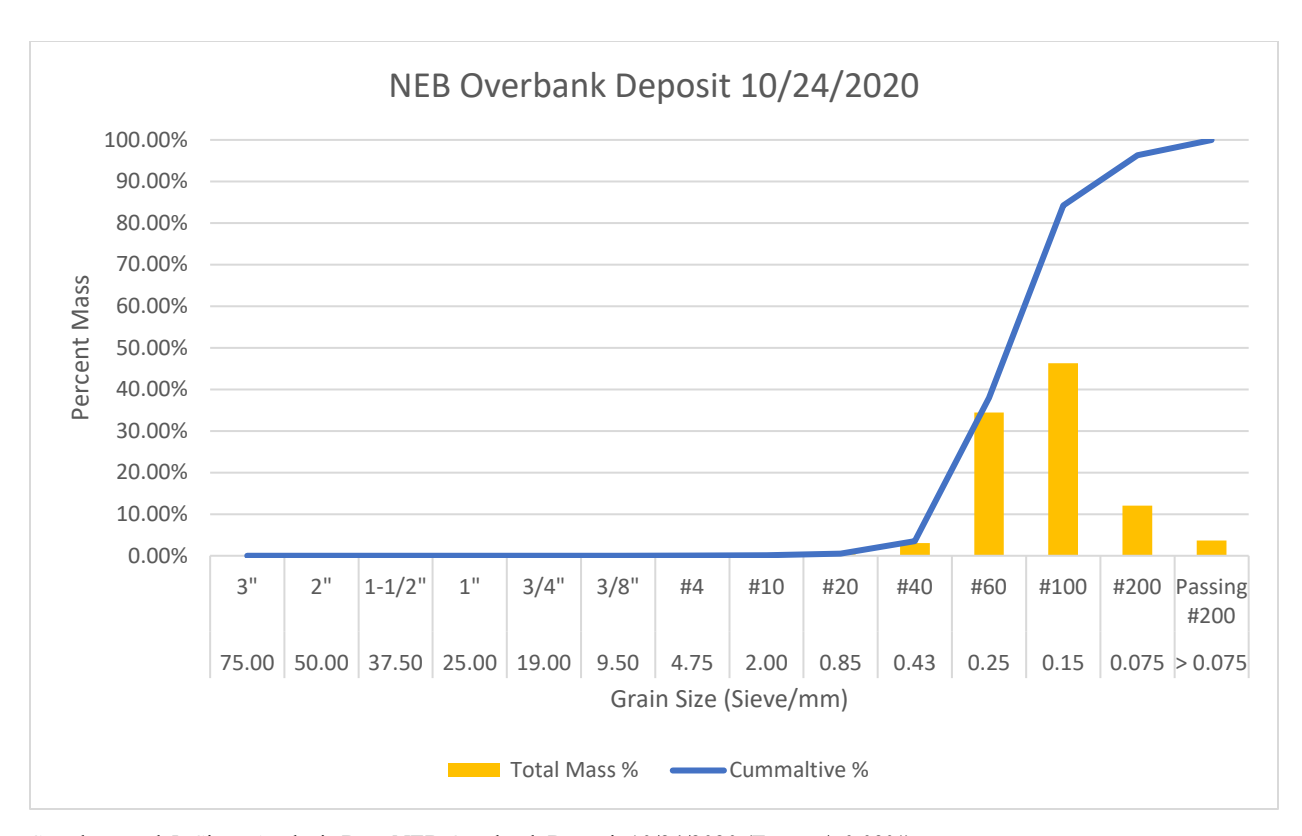
Supplemental 2: Stream geometry data for the Northwest Branch (April 2015- October 2020)

| Date             | 0            | Width | Area              | Donth     | Velocity | Shear Stress        | T*    |
|------------------|--------------|-------|-------------------|-----------|----------|---------------------|-------|
| Date             | Q<br>(m^3/s) | (m)   | (m <sup>2</sup> ) | Depth (m) | (m/s)    | (N/m <sup>2</sup> ) | 1 **  |
| 2/2/2010 11:44   | 1.53         | 20.42 | 6.44              | 0.32      | 0.24     | 12.18               | 0.025 |
| 3/31/2010 14:01  | 2.86         | 19.96 | 8.70              | 0.44      | 0.33     | 16.83               | 0.035 |
| 5/12/2010 11:45  | 1.13         | 19.81 | 6.85              | 0.35      | 0.16     | 13.35               | 0.027 |
| 6/29/2010 11:57  | 1.51         | 20.12 | 7.01              | 0.35      | 0.22     | 13.47               | 0.028 |
| 7/9/2010 10:05   | 0.27         | 19.57 | 4.12              | 0.21      | 0.07     | 8.13                | 0.017 |
| 8/26/2010 14:50  | 0.69         | 20.12 | 7.22              | 0.36      | 0.10     | 13.86               | 0.029 |
| 10/13/2010 11:52 | 0.53         | 20.42 | 3.75              | 0.18      | 0.14     | 7.10                | 0.015 |
| 12/9/2010 13:39  | 0.74         | 19.05 | 4.76              | 0.25      | 0.16     | 9.65                | 0.020 |
| 2/9/2011 13:29   | 1.62         | 20.42 | 4.52              | 0.22      | 0.36     | 8.54                | 0.018 |
| 3/7/2011 11:44   | 12.74        | 22.86 | 14.68             | 0.64      | 0.87     | 24.81               | 0.051 |
| 4/14/2011 11:52  | 2.12         | 20.57 | 6.61              | 0.32      | 0.32     | 12.40               | 0.026 |
| 5/31/2011 8:50   | 0.57         | 20.67 | 3.62              | 0.18      | 0.16     | 6.77                | 0.014 |
| 7/25/2011 11:49  | 0.21         | 20.12 | 2.97              | 0.15      | 0.07     | 5.71                | 0.012 |
| 8/28/2011 10:24  | 85.80        | 30.02 | 47.94             | 1.60      | 1.72     | 61.69               | 0.127 |
| 10/6/2011 12:41  | 1.01         | 17.98 | 7.56              | 0.42      | 0.13     | 16.25               | 0.033 |
| 12/21/2011 11:14 | 1.15         | 21.49 | 5.24              | 0.24      | 0.22     | 9.42                | 0.019 |
| 2/7/2012 13:20   | 1.23         | 20.42 | 6.35              | 0.31      | 0.19     | 12.02               | 0.025 |
| 2/28/2012 9:42   | 0.95         | 20.42 | 6.02              | 0.29      | 0.16     | 11.39               | 0.023 |
| 3/1/2012 8:31    | 15.94        | 22.56 | 18.49             | 0.82      | 0.86     | 31.67               | 0.065 |
| 4/9/2012 12:04   | 0.73         | 20.57 | 4.47              | 0.22      | 0.16     | 8.39                | 0.017 |
| 6/11/2012 14:22  | 0.44         | 20.42 | 4.89              | 0.24      | 0.09     | 9.25                | 0.019 |
| 8/1/2012 13:04   | 0.28         | 19.81 | 4.13              | 0.21      | 0.07     | 8.06                | 0.017 |
| 9/17/2012 13:52  | 0.17         | 18.90 | 3.34              | 0.18      | 0.05     | 6.84                | 0.014 |
| 10/9/2012 13:27  | 0.65         | 19.69 | 4.52              | 0.23      | 0.14     | 8.86                | 0.018 |
| 12/3/2012 10:33  | 0.57         | 17.77 | 4.54              | 0.26      | 0.12     | 9.88                | 0.020 |
| 2/11/2013 10:34  | 6.85         | 21.55 | 9.66              | 0.45      | 0.71     | 17.32               | 0.036 |
| 4/16/2013 10:59  | 0.91         | 17.50 | 6.58              | 0.38      | 0.14     | 14.53               | 0.030 |
| 6/10/2013 10:39  | 13.39        | 26.52 | 14.40             | 0.54      | 0.93     | 20.98               | 0.043 |
| 6/20/2013 14:07  | 0.85         | 19.26 | 4.91              | 0.25      | 0.17     | 9.84                | 0.020 |
| 8/21/2013 9:15   | 0.33         | 17.74 | 6.51              | 0.37      | 0.05     | 14.18               | 0.029 |
| 10/31/2013 10:33 | 0.54         | 16.92 | 10.41             | 0.62      | 0.05     | 23.77               | 0.049 |
| 12/13/2013 10:12 | 1.44         | 20.33 | 3.33              | 0.16      | 0.43     | 6.32                | 0.013 |
| 3/5/2014 13:26   | 2.65         | 18.59 | 10.78             | 0.58      | 0.25     | 22.40               | 0.046 |
| 4/23/2014 12:59  | 1.82         | 17.47 | 12.08             | 0.69      | 0.15     | 26.72               | 0.055 |
| 6/18/2014 11:36  | 0.95         | 19.39 | 5.64              | 0.29      | 0.17     | 11.24               | 0.023 |
| 8/19/2014 13:46  | 0.52         | 19.05 | 3.58              | 0.19      | 0.15     | 7.25                | 0.015 |
| 10/20/2014 13:40 | 0.61         | 18.75 | 3.85              | 0.21      | 0.16     | 7.93                | 0.016 |
| 12/2/2014 15:05  | 5.92         | 19.87 | 10.96             | 0.55      | 0.54     | 21.31               | 0.044 |

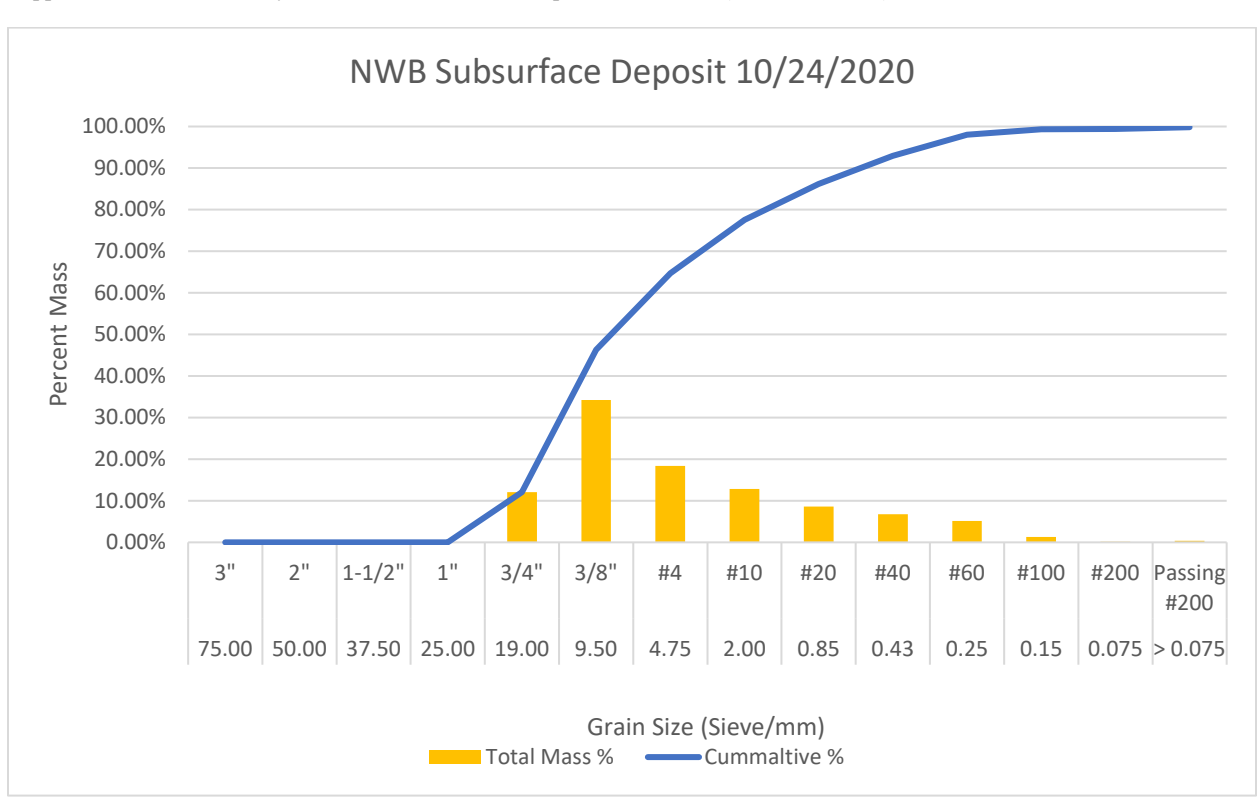
Supplemental 3: Stream geometry data for the Northeast Branch (February 2010- December 2014)

| Date             | Q       | Width | Area  | Depth | Velocity | Shear Stress | T*    |
|------------------|---------|-------|-------|-------|----------|--------------|-------|
|                  | (m^3/s) | (m)   | (m^2) | (m)   | (m/s)    | (N/m^2)      |       |
| 2/4/2015 14:48   | 1.42    | 20.18 | 6.09  | 0.30  | 0.23     | 11.67        | 0.024 |
| 4/29/2015 10:24  | 1.50    | 19.93 | 4.76  | 0.24  | 0.31     | 9.22         | 0.019 |
| 6/10/2015 13:13  | 1.72    | 19.99 | 4.55  | 0.23  | 0.38     | 8.80         | 0.018 |
| 8/17/2015 12:12  | 0.39    | 18.90 | 6.25  | 0.33  | 0.06     | 12.78        | 0.026 |
| 10/7/2015 13:36  | 0.81    | 19.60 | 6.39  | 0.33  | 0.13     | 12.60        | 0.026 |
| 11/30/2015 12:17 | 0.99    | 17.19 | 8.55  | 0.50  | 0.12     | 19.21        | 0.040 |
| 2/2/2016 11:20   | 9.60    | 26.24 | 11.71 | 0.45  | 0.82     | 17.23        | 0.035 |
| 2/10/2016 9:53   | 2.97    | 22.25 | 6.94  | 0.31  | 0.43     | 12.05        | 0.025 |
| 2/25/2016 9:22   | 33.13   | 30.24 | 27.87 | 0.92  | 1.19     | 35.62        | 0.073 |
| 4/8/2016 13:49   | 3.20    | 16.06 | 12.73 | 0.79  | 0.25     | 30.62        | 0.063 |
| 6/8/2016 12:01   | 0.70    | 21.18 | 3.67  | 0.17  | 0.19     | 6.69         | 0.014 |
| 7/7/2016 11:17   | 1.04    | 20.36 | 5.21  | 0.26  | 0.20     | 9.89         | 0.020 |
| 7/19/2016 8:29   | 1.69    | 19.90 | 7.37  | 0.37  | 0.23     | 14.30        | 0.029 |
| 10/6/2016 14:58  | 0.48    | 18.78 | 3.79  | 0.20  | 0.13     | 7.80         | 0.016 |
| 12/7/2016 9:38   | 4.59    | 26.76 | 6.89  | 0.26  | 0.66     | 9.95         | 0.020 |
| 2/6/2017 14:41   | 0.67    | 17.43 | 7.65  | 0.44  | 0.09     | 16.94        | 0.035 |
| 4/11/2017 13:24  | 1.13    | 18.59 | 5.64  | 0.30  | 0.20     | 11.72        | 0.024 |
| 6/21/2017 11:53  | 0.53    | 18.71 | 4.63  | 0.25  | 0.11     | 9.55         | 0.020 |
| 7/24/2017 10:41  | 11.75   | 24.78 | 13.47 | 0.54  | 0.87     | 21.00        | 0.043 |
| 7/24/2017 11:17  | 10.96   | 22.92 | 14.68 | 0.64  | 0.75     | 24.74        | 0.051 |
| 8/8/2017 13:05   | 3.17    | 26.06 | 5.22  | 0.20  | 0.61     | 7.74         | 0.016 |
| 8/24/2017 13:31  | 0.71    | 17.89 | 5.98  | 0.33  | 0.12     | 12.92        | 0.027 |
| 8/24/2017 14:06  | 0.71    | 18.14 | 5.93  | 0.33  | 0.12     | 12.63        | 0.026 |
| 9/28/2017 14:49  | 0.71    | 18.90 | 4.74  | 0.33  | 0.12     | 9.69         | 0.020 |
| 9/28/2017 15:02  | 0.43    | 18.75 | 4.88  | 0.25  | 0.09     | 10.05        | 0.020 |
| 10/18/2017 15:10 | 0.53    | 19.05 | 5.15  | 0.20  | 0.10     | 10.44        | 0.021 |
| 12/14/2017 15:11 | 0.57    | 18.59 | 4.55  | 0.27  | 0.10     | 9.46         | 0.021 |
|                  | 1.95    | 20.39 | 5.81  | 0.24  | 0.12     | 11.00        | 0.019 |
| 2/26/2018 12:46  | 0.68    |       | 5.65  | 0.28  |          | 11.55        | 0.023 |
| 4/13/2018 13:58  |         | 18.90 | _     |       | 0.12     | _            |       |
| 4/20/2018 9:30   | 1.34    | 18.87 | 6.08  | 0.32  | 0.22     | 12.44        | 0.026 |
| 6/4/2018 10:51   | 28.12   | 29.32 | 27.69 | 0.94  | 1.01     | 36.48        | 0.075 |
| 6/19/2018 10:14  | 0.73    | 16.89 | 6.21  | 0.37  | 0.12     | 14.20        | 0.029 |
| 8/14/2018 10:04  | 1.59    | 24.17 | 7.32  | 0.30  | 0.22     | 11.70        | 0.024 |
| 10/9/2018 11:15  | 1.23    | 20.18 | 5.33  | 0.26  | 0.23     | 10.21        | 0.021 |
| 11/6/2018 13:58  | 59.18   | 27.43 | 36.60 | 1.33  | 1.62     | 51.56        | 0.106 |
| 12/10/2018 9:59  | 1.59    | 20.12 | 4.37  | 0.22  | 0.36     | 8.39         | 0.017 |
| 2/4/2019 9:34    | 1.94    | 20.82 | 6.39  | 0.31  | 0.30     | 11.86        | 0.024 |
| 4/24/2019 8:58   | 1.31    | 21.34 | 4.12  | 0.19  | 0.32     | 7.45         | 0.015 |
| 6/19/2019 10:36  | 1.80    | 20.18 | 5.34  | 0.26  | 0.34     | 10.23        | 0.021 |
| 8/22/2019 13:49  | 1.80    | 19.08 | 6.61  | 0.35  | 0.27     | 13.39        | 0.028 |
| 9/18/2019 14:32  | 0.31    | 19.20 | 3.36  | 0.18  | 0.09     | 6.77         | 0.014 |
| 10/8/2019 13:31  | 0.26    | 18.84 | 3.53  | 0.19  | 0.07     | 7.24         | 0.015 |
| 12/19/2019 11:05 | 1.40    | 18.75 | 7.05  | 0.38  | 0.20     | 14.53        | 0.030 |
| 2/11/2020 13:11  | 17.22   | 28.19 | 17.56 | 0.62  | 0.98     | 24.06        | 0.050 |
| 3/27/2020 8:41   | 1.57    | 19.39 | 7.47  | 0.39  | 0.21     | 14.89        | 0.031 |
| 4/22/2020 8:44   | 1.23    | 18.96 | 7.39  | 0.39  | 0.17     | 15.05        | 0.031 |
| 5/28/2020 8:41   | 0.94    | 19.20 | 8.12  | 0.42  | 0.12     | 16.34        | 0.034 |
| 8/10/2020 10:32  | 1.29    | 20.57 | 5.15  | 0.25  | 0.25     | 9.67         | 0.020 |
| 9/17/2020 12:33  | 1.14    | 20.18 | 5.69  | 0.28  | 0.20     | 10.89        | 0.022 |
| 10/2/2020 9:55   | 2.31    | 20.03 | 8.93  | 0.45  | 0.26     | 17.23        | 0.035 |

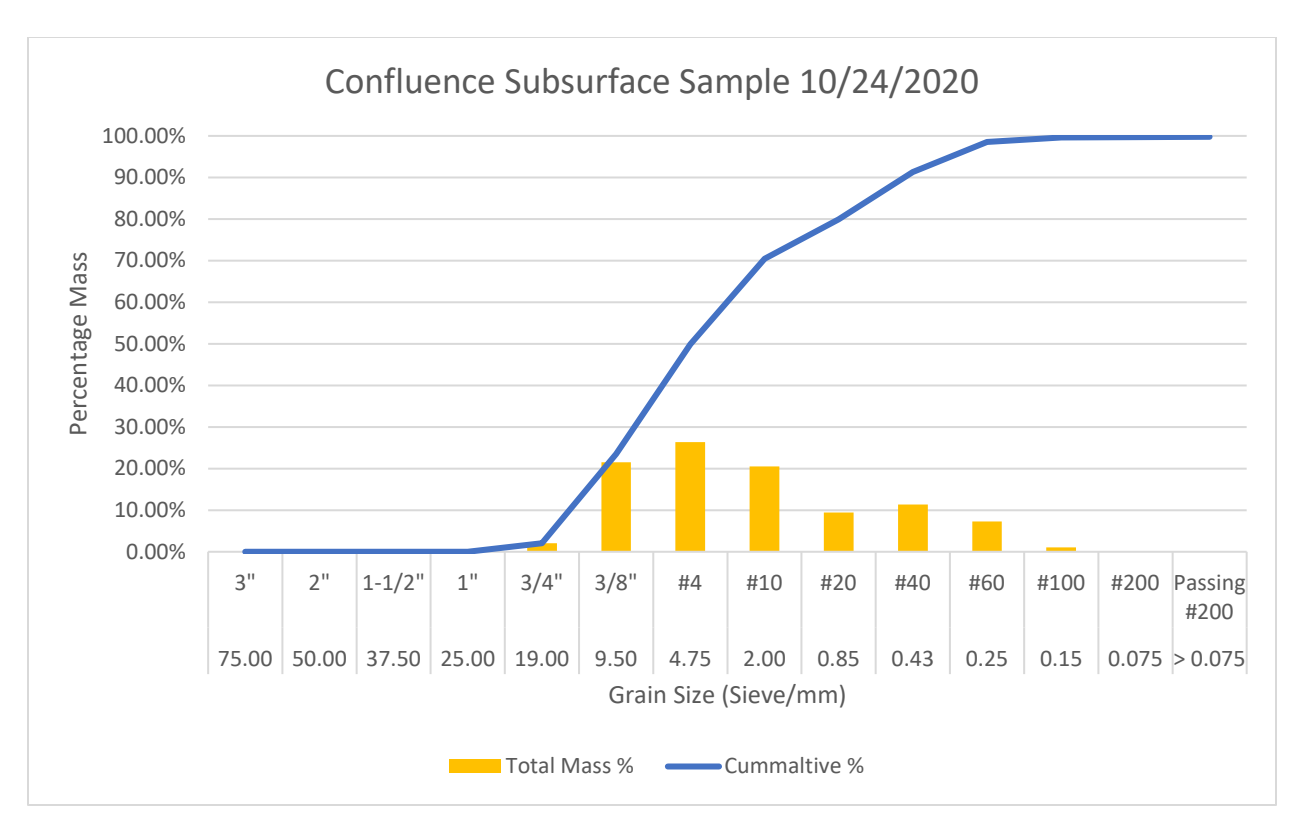
Supplemental 4: Stream geometry data Northeast Branch (February 2015- October 2020)



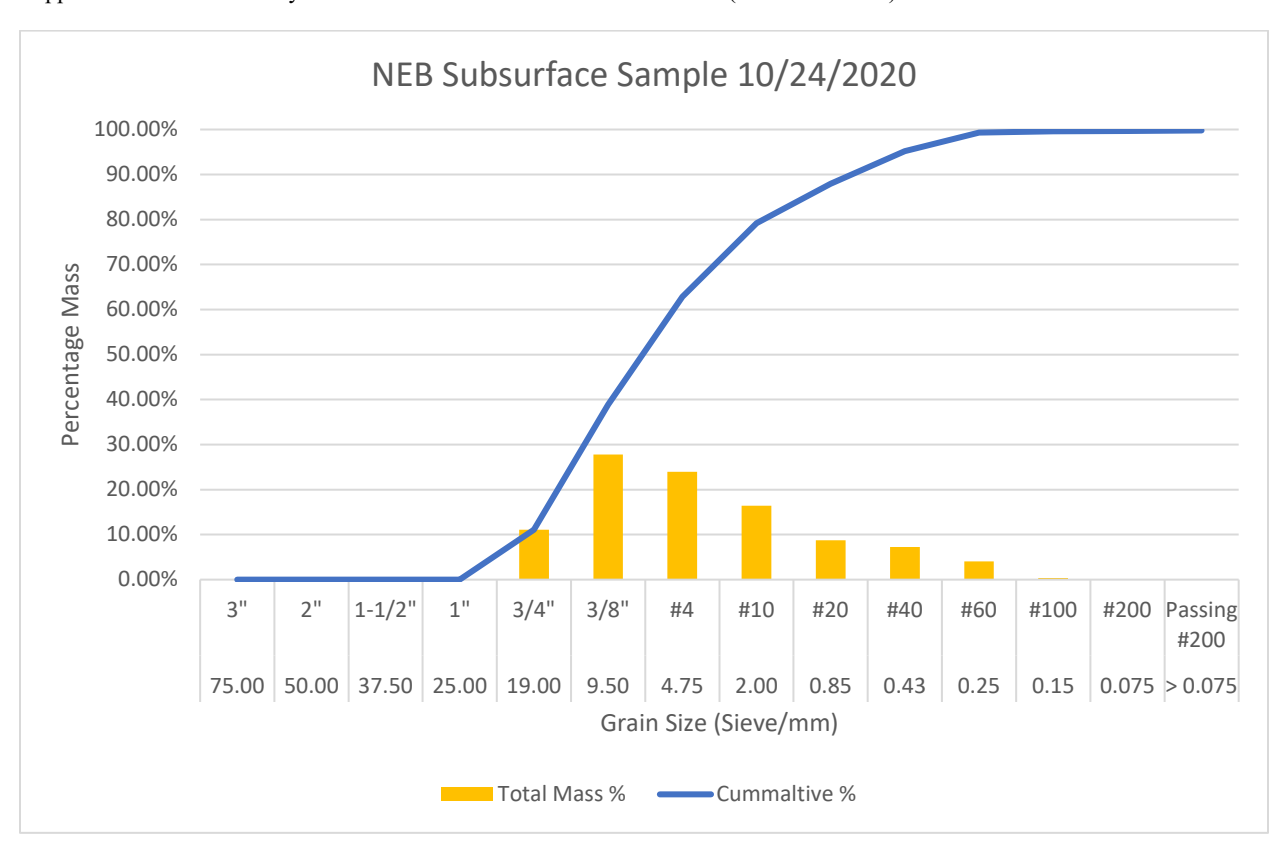
Supplemental 5: Sieve Analysis Data NEB Overbank Deposit 10/24/2020 (Error +/- 0.03%)



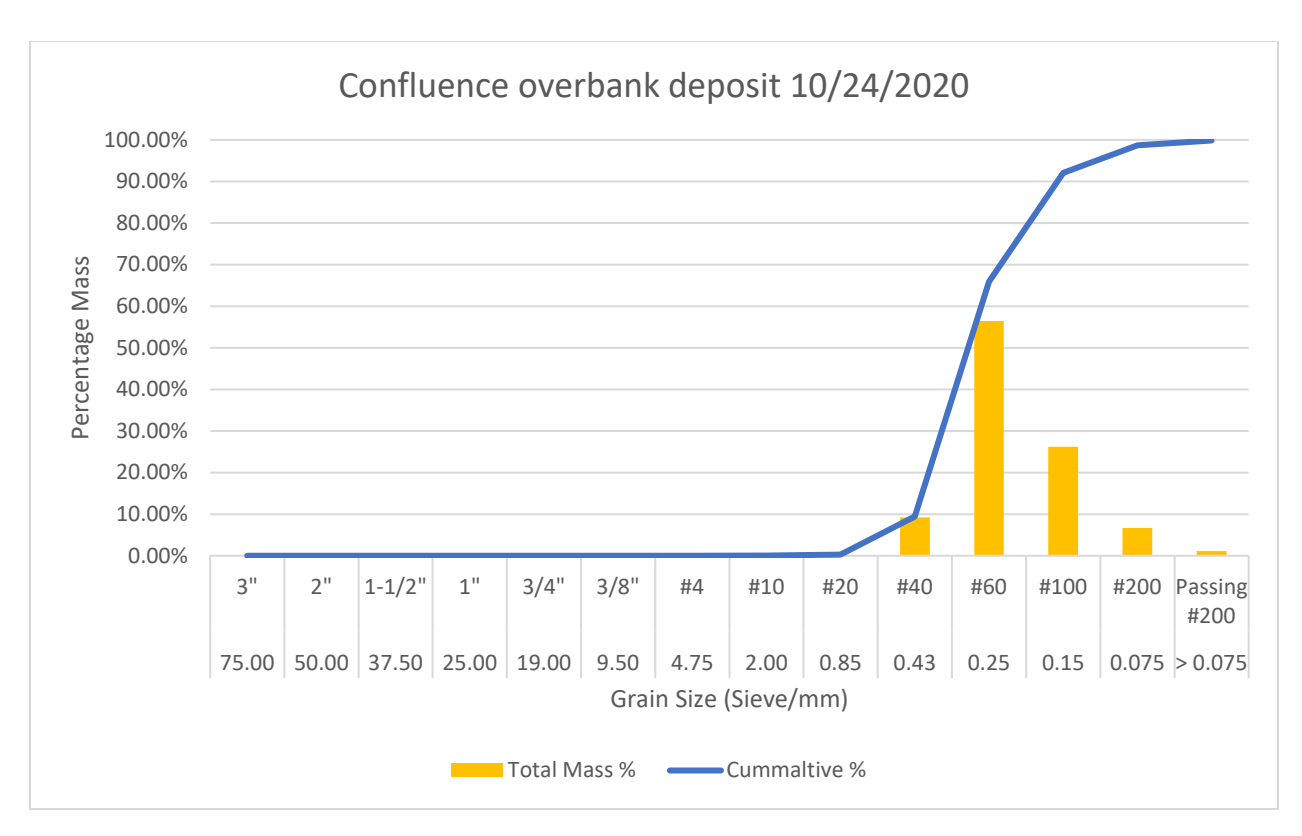
Supplemental 6: Sieve Analysis Data NWB Subsurface 10/24/2020 (Error +/- 0.17%)



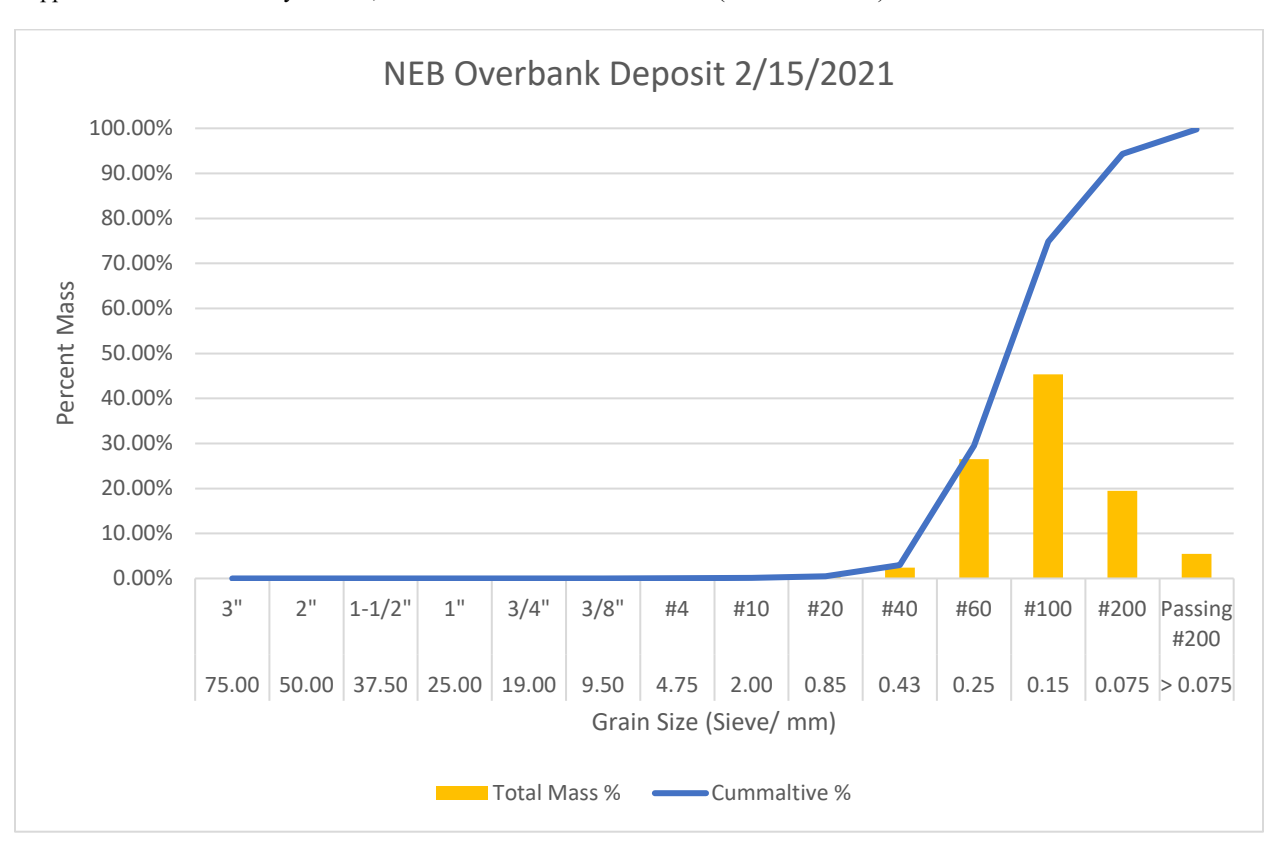
Supplemental 7: Sieve Analysis Data Confluence Subsurface 10/24/2020 (Error +/- 0.21%)



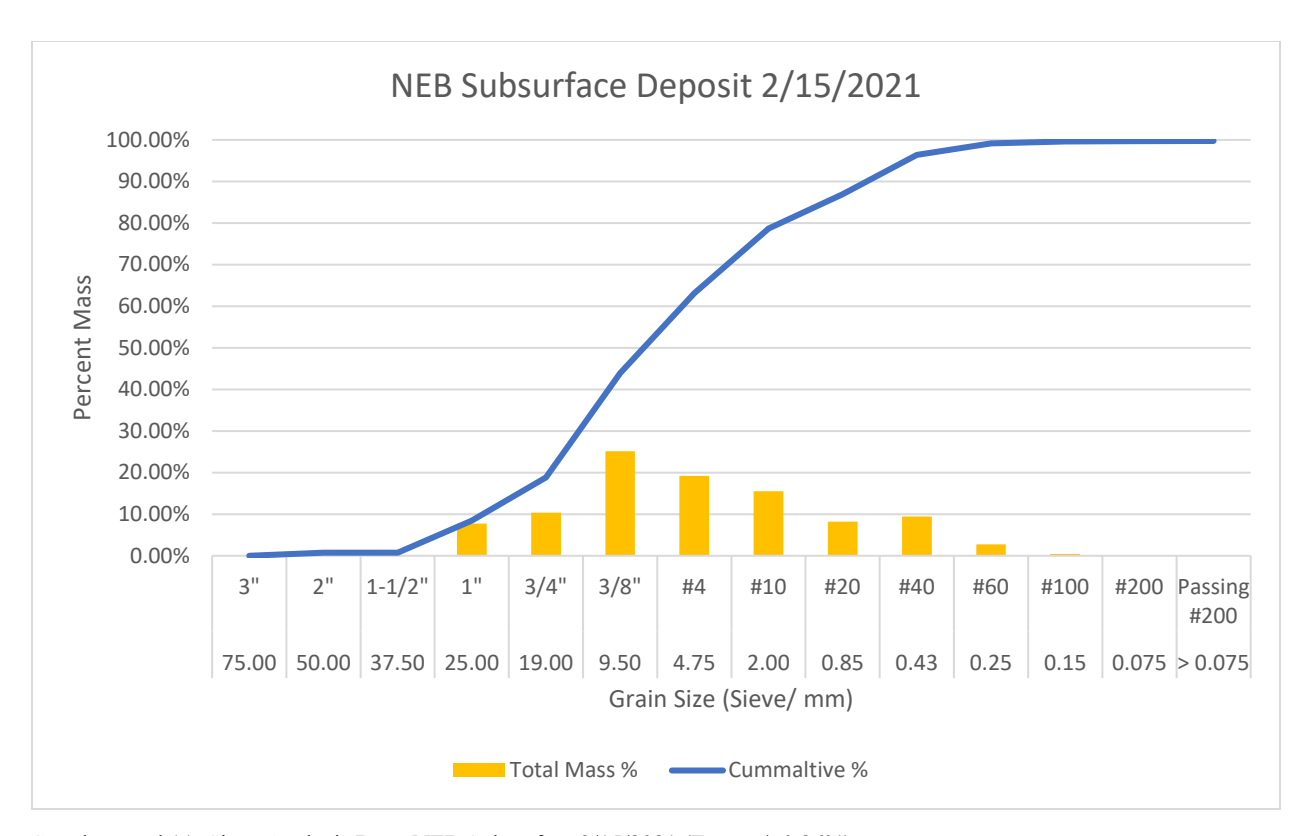
Supplemental 8: Sieve Analysis NEB Subsurface Sample 10/24/2020 (Error +/- 0.21%)



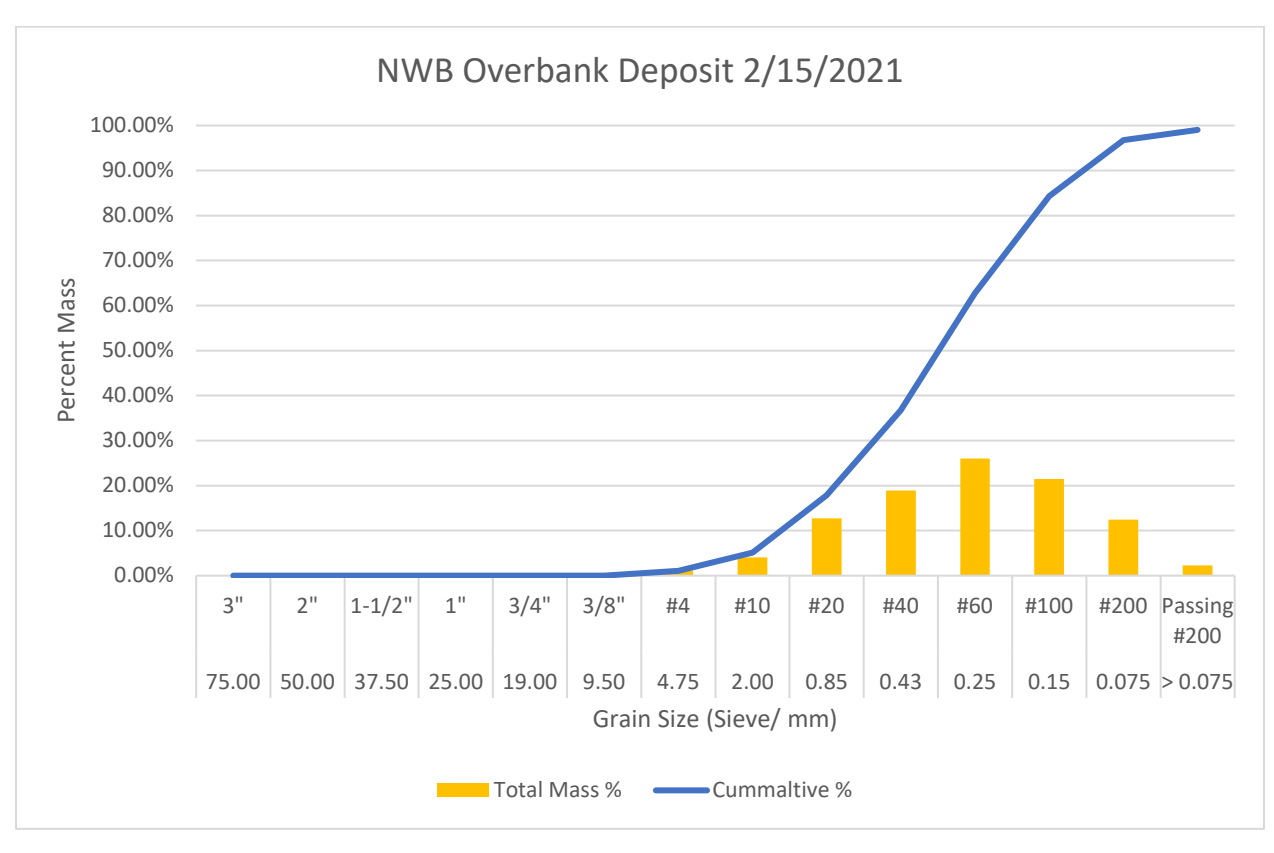
Supplemental 9: Sieve Analysis Data, Confluence Overbank 10/24/2020 (Error +/- 0.12%)



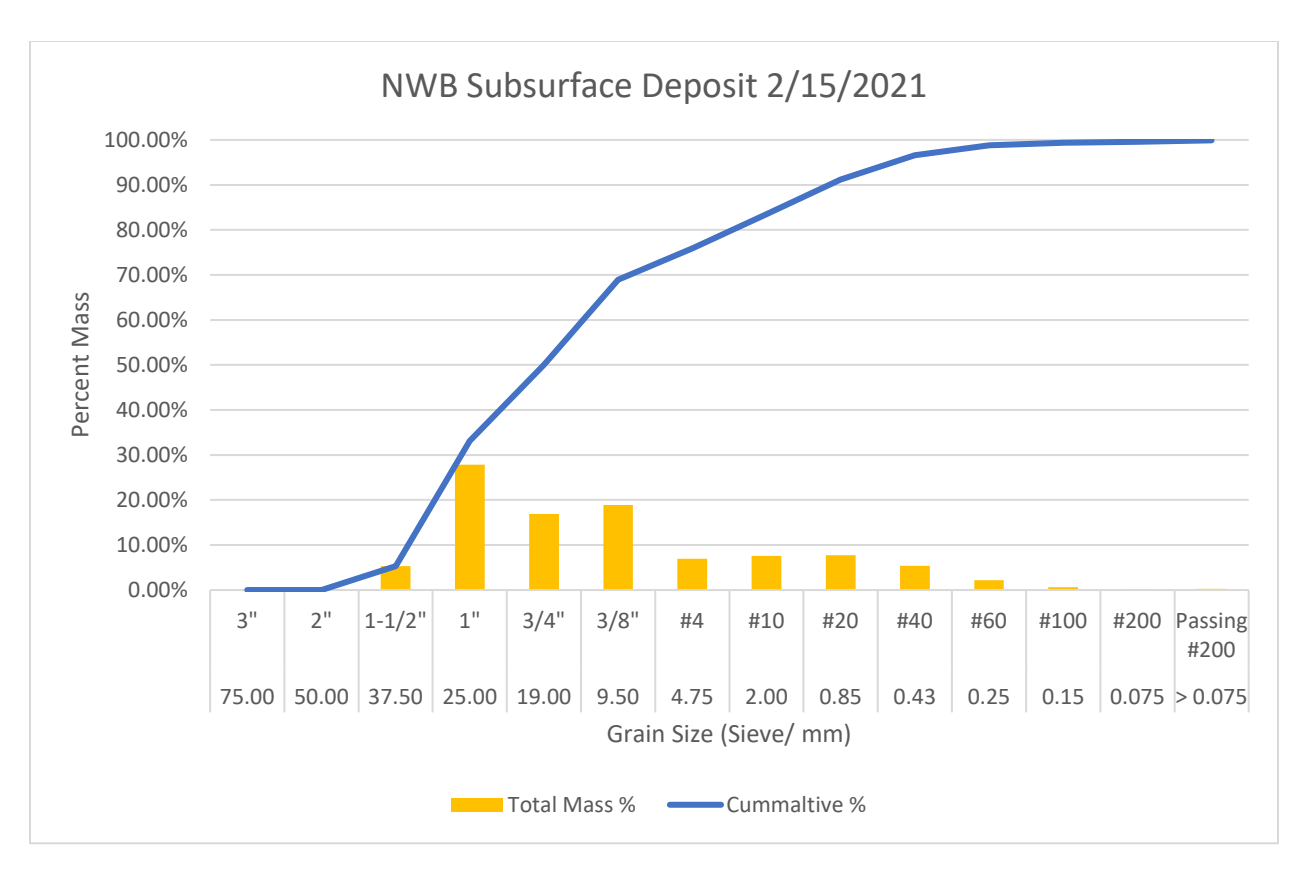
Supplemental 10: Sieve Analysis Data, NEB Overbank 2/15/2021 (Error +/- 0.23%)



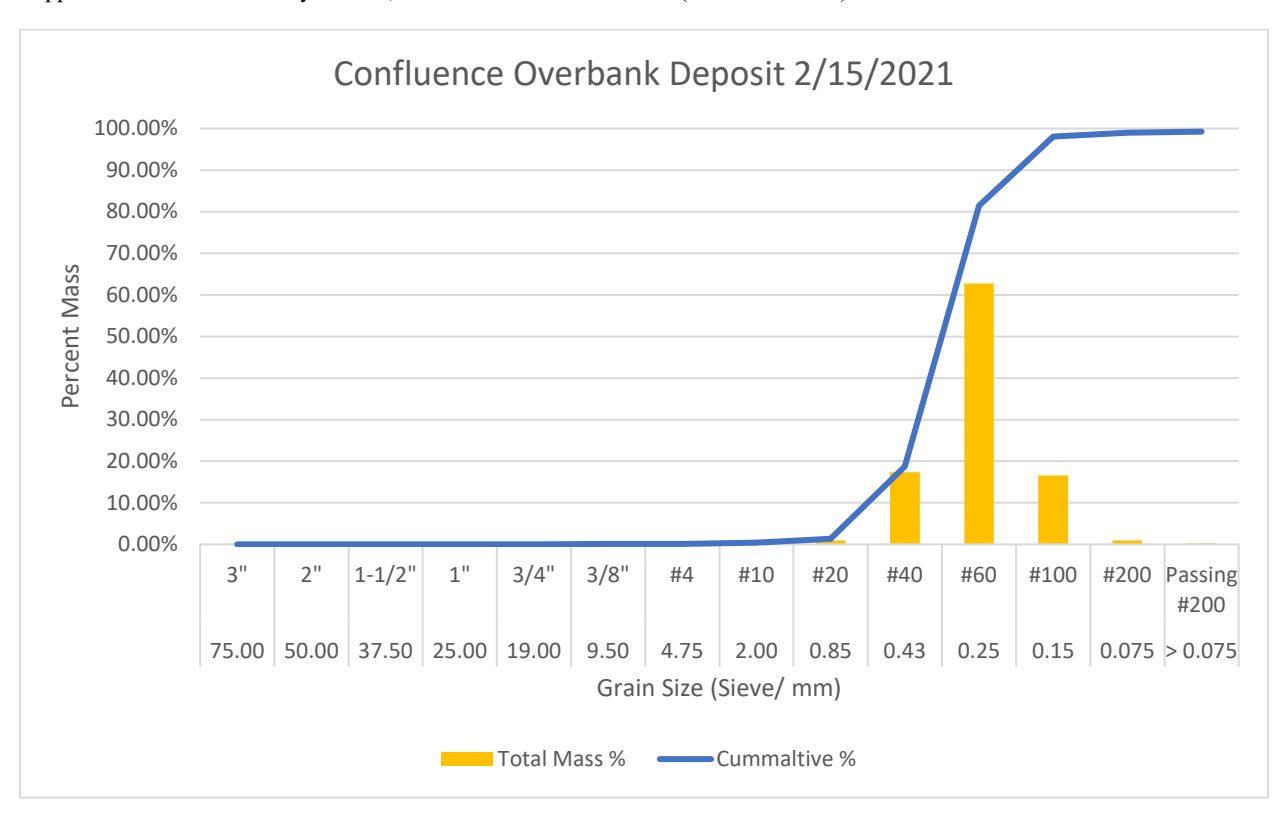
Supplemental 11: Sieve Analysis Data, NEB Subsurface 2/15/2021 (Error +/- 0.26%)



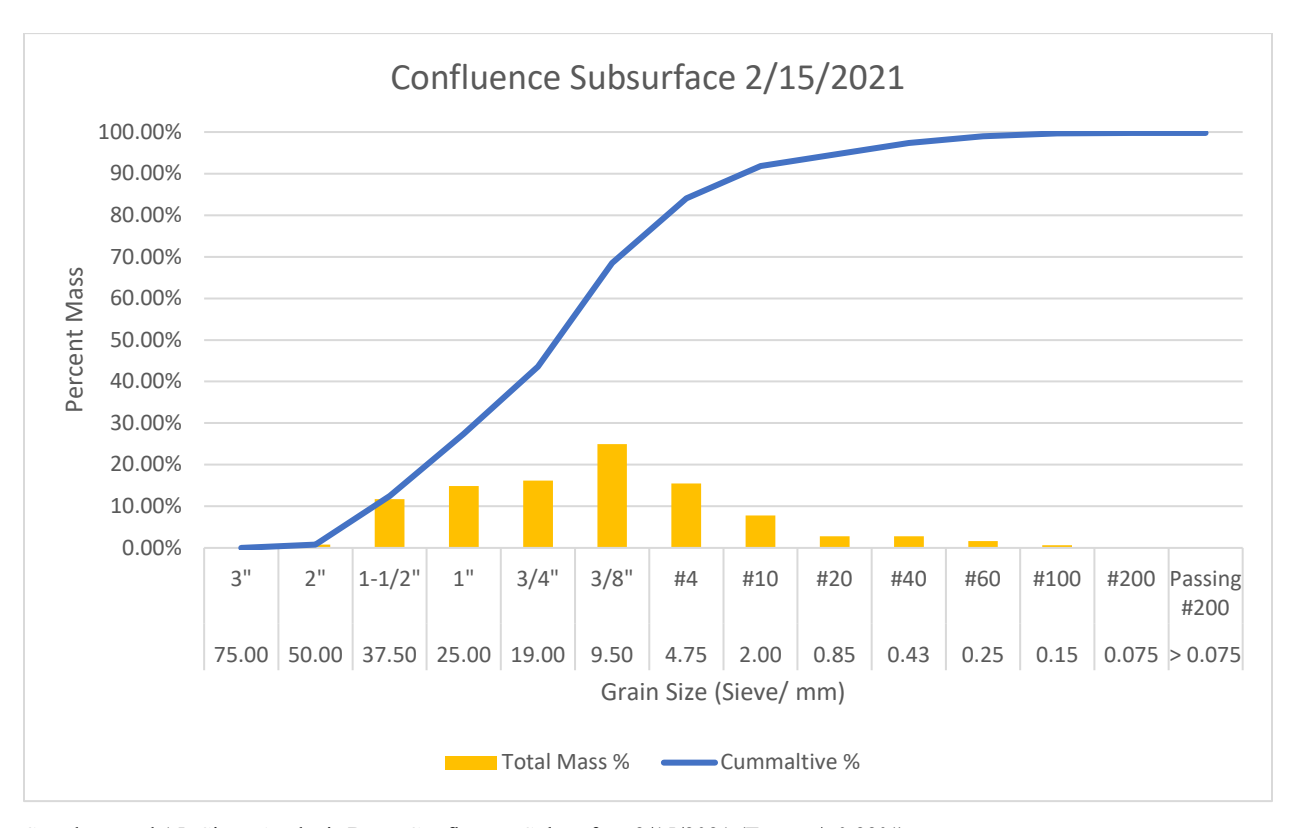
Supplemental 12: Sieve Analysis Data, NWB Overbank 2/15/2021 (Error 0.98%)



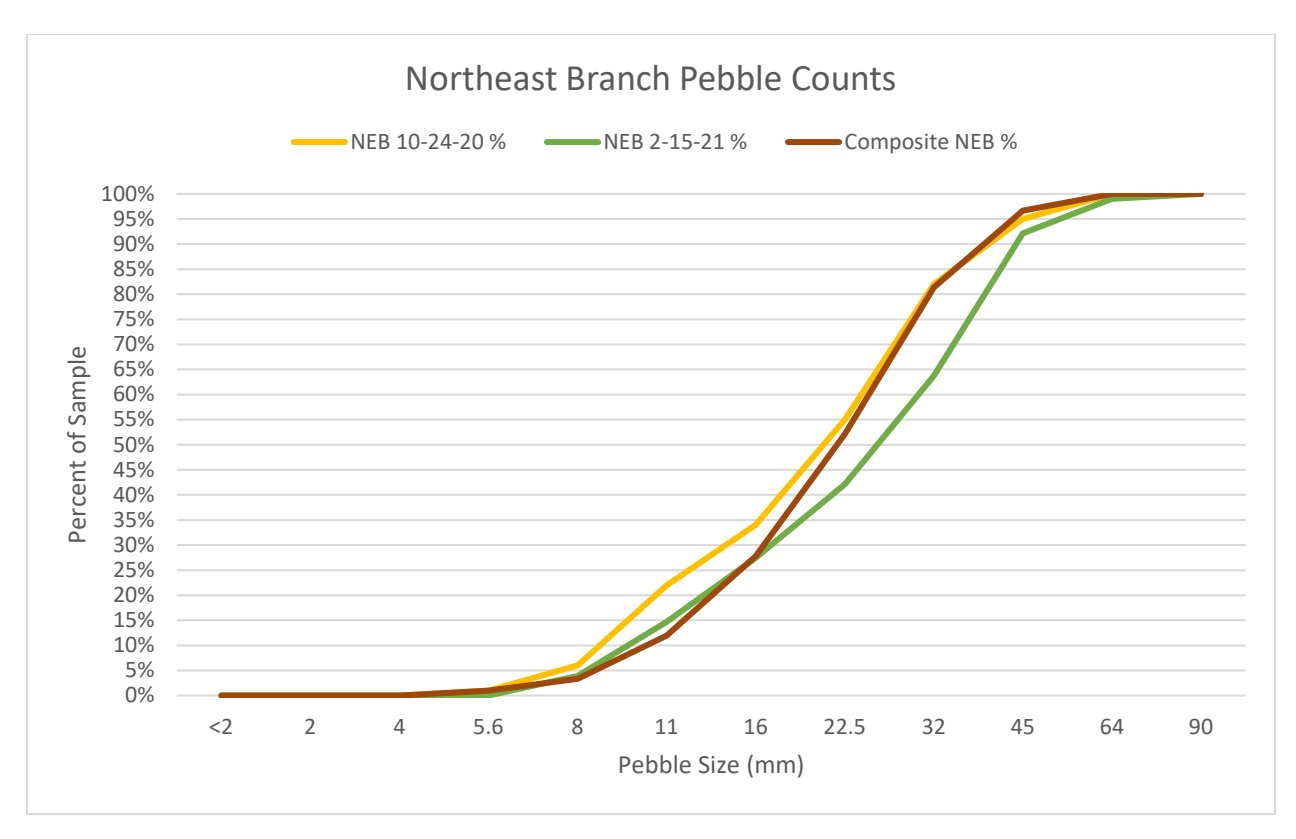
Supplemental 13: Sieve Analysis Data, NWB Subsurface 2/15/2021 (Error +/- 0.98%)



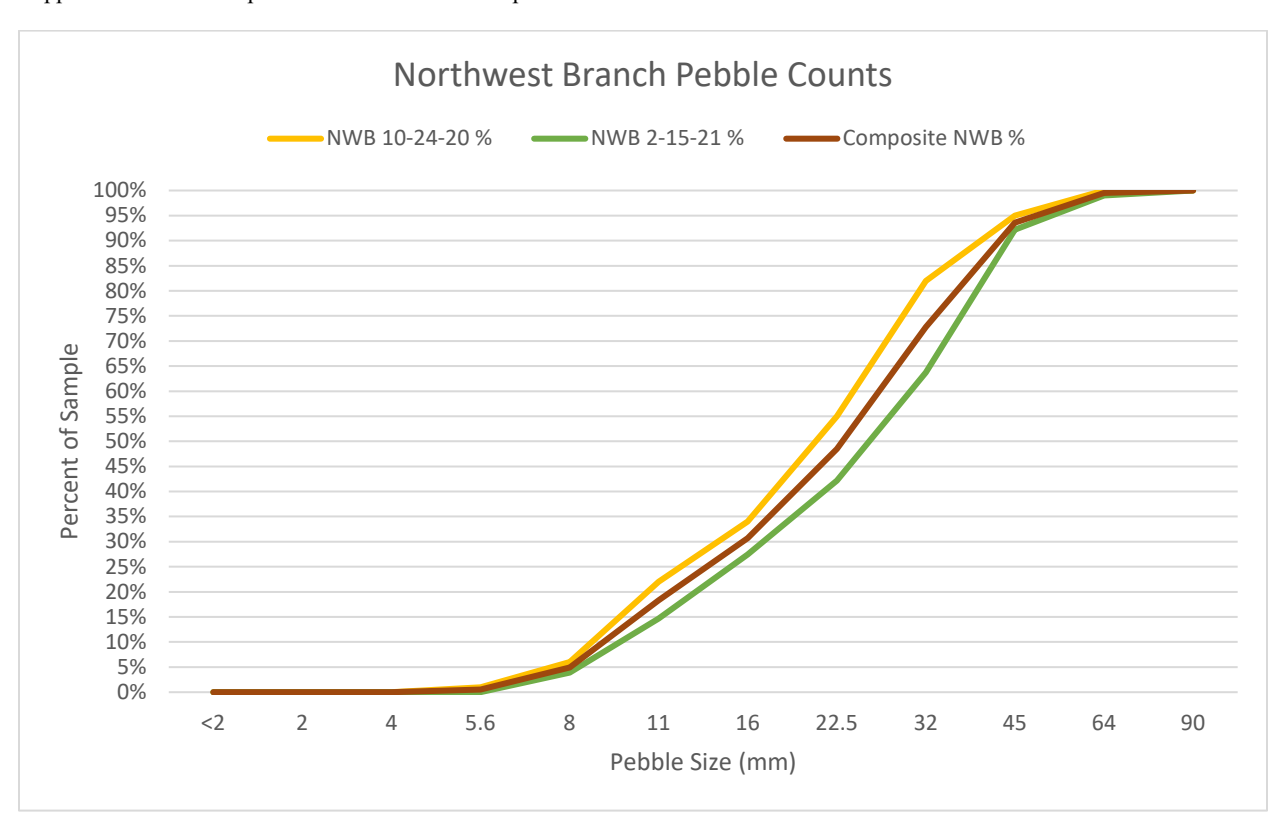
Supplemental 14: Sieve Analysis Data, Confluence Overbank 2/15/2021 (Error +/- 0.75%)



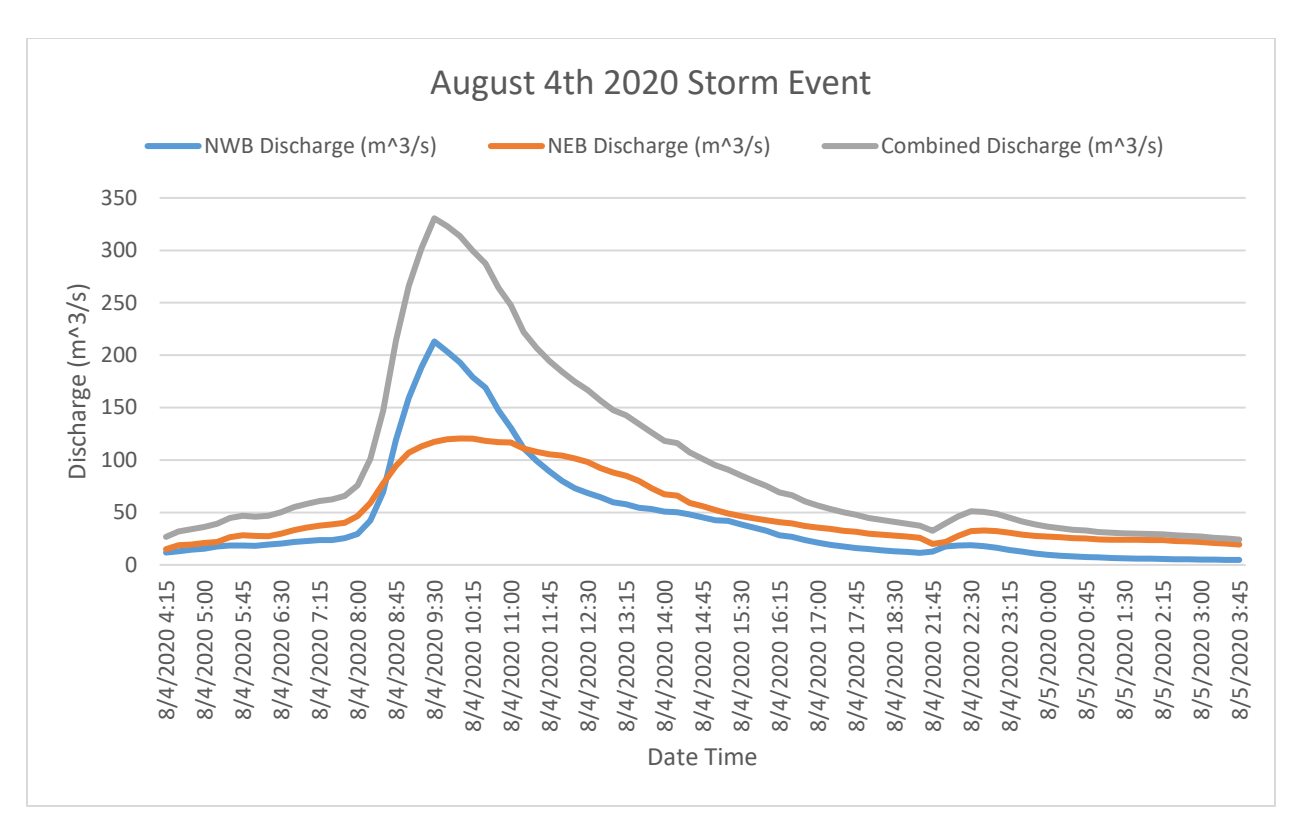
Supplemental 15: Sieve Analysis Data, Confluence Subsurface 2/15/2021 (Error +/- 0.22%)



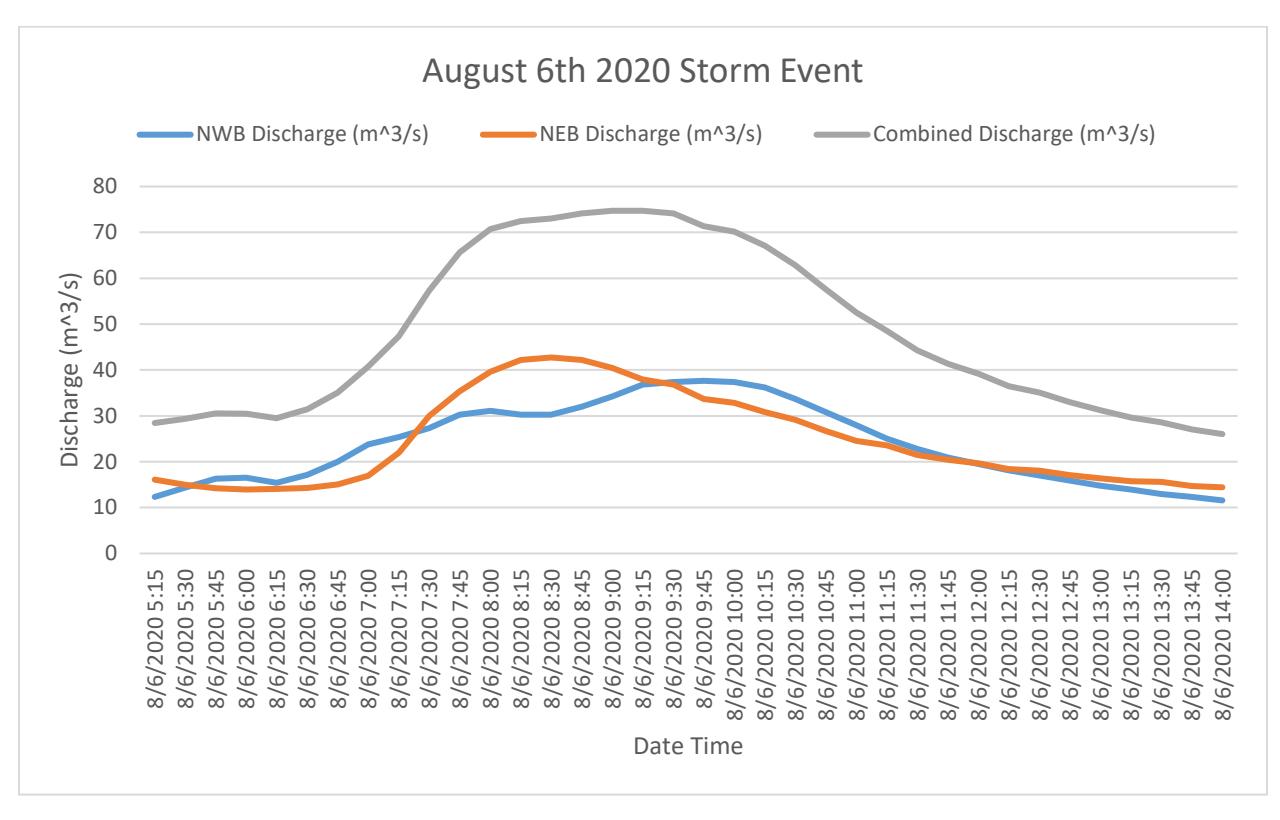
Supplemental 16: NEB pebble count data with composite line



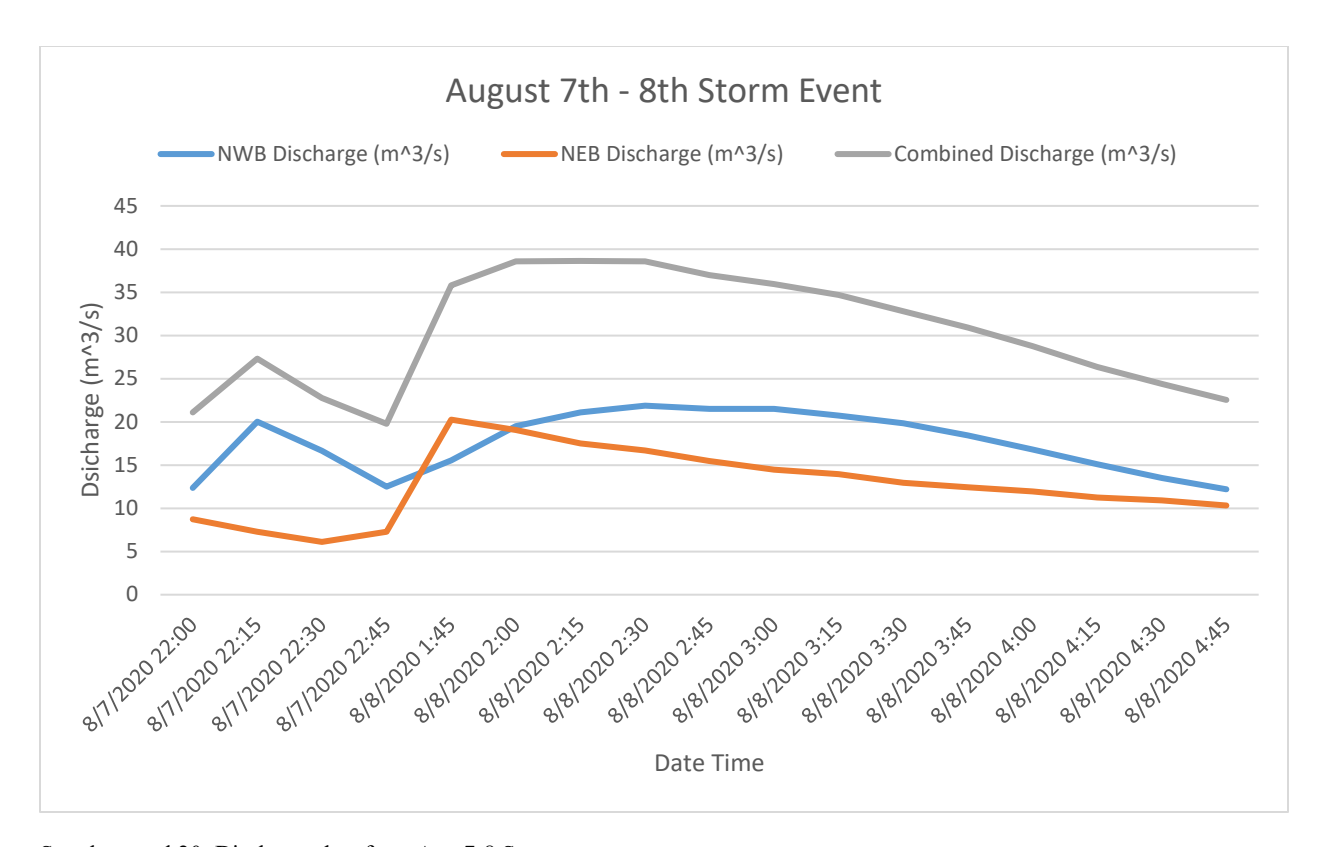
Supplemental 17: NWB pebble count data with composite line



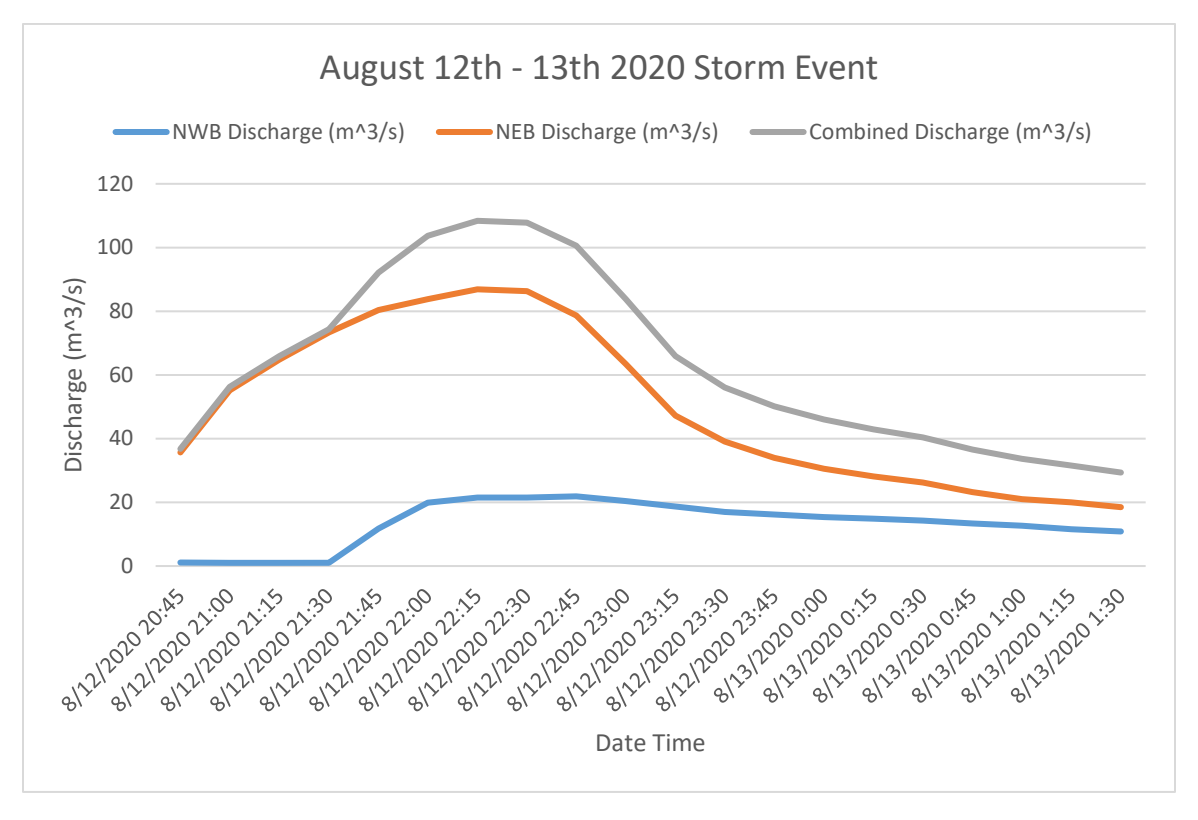
Supplemental 18: Discharge data from Aug 4th 2020 Storm Event



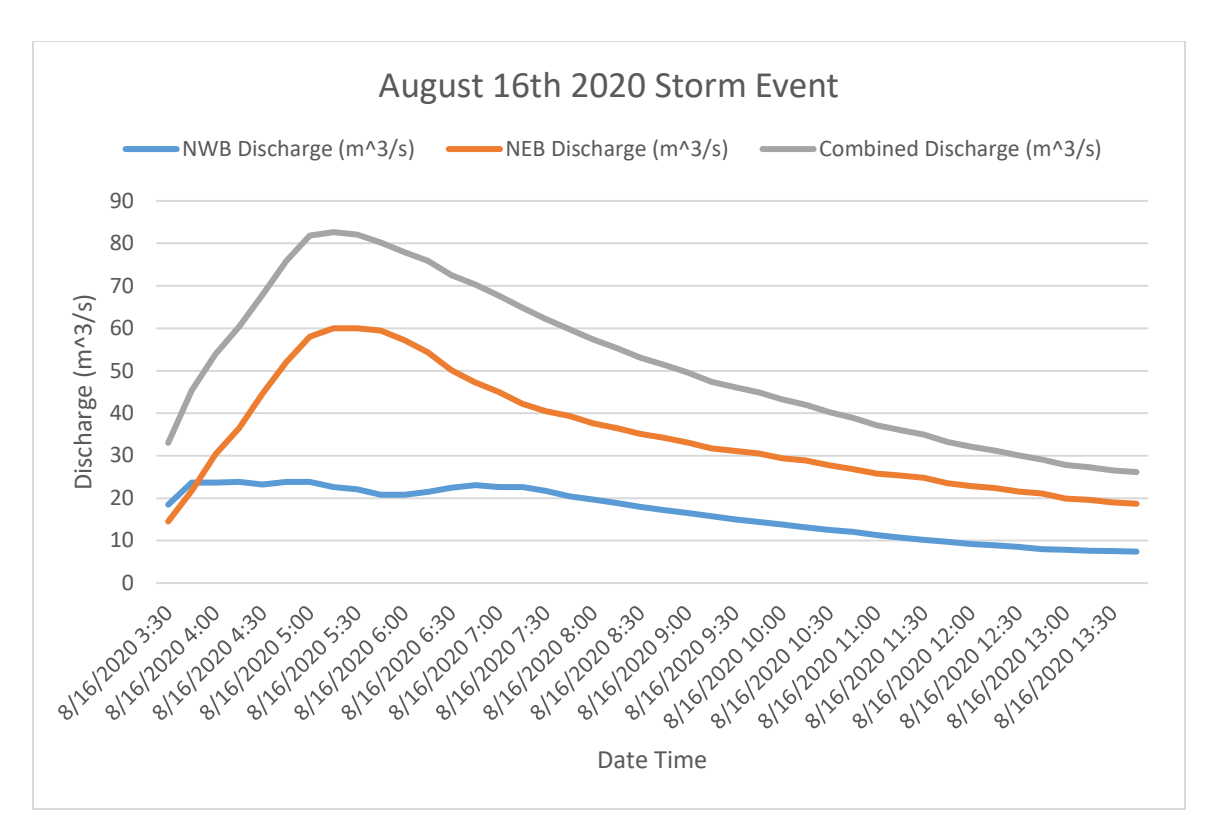
Supplemental 19: Discharge data from Aug 6th 2020 Storm Event



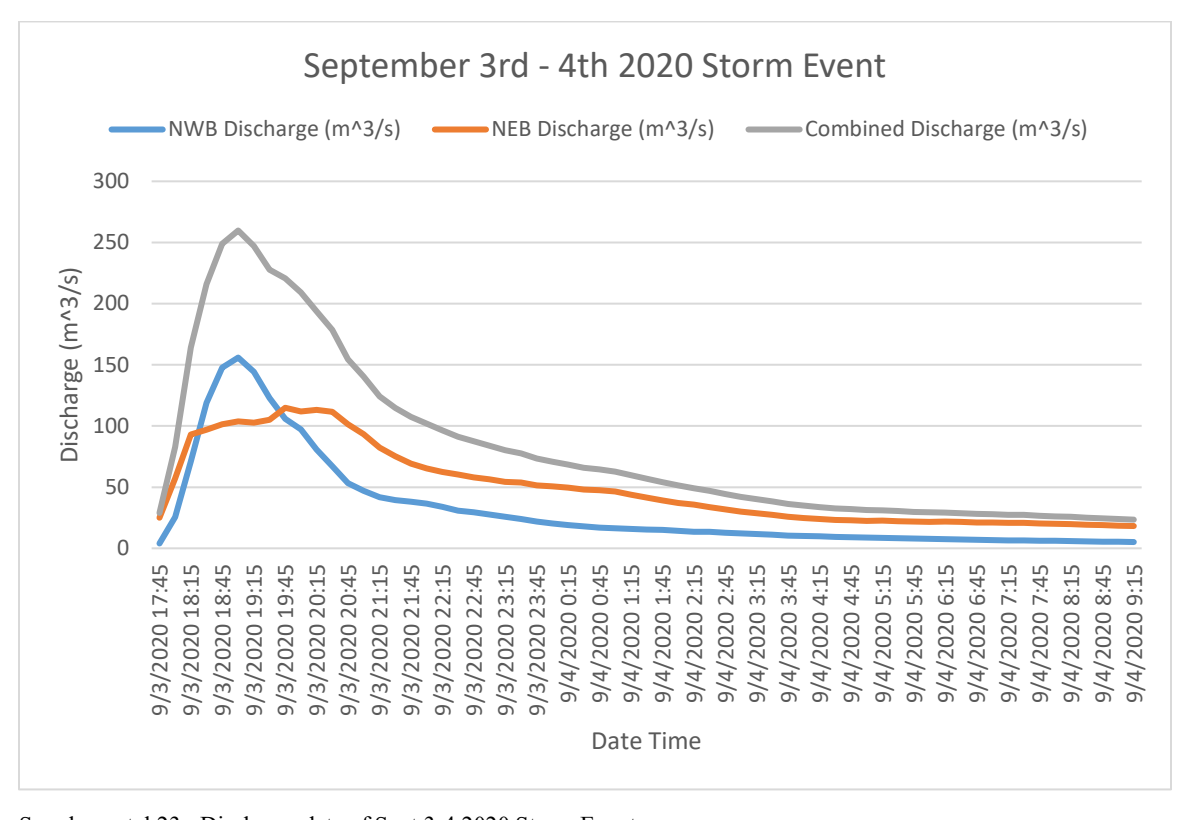
Supplemental 20: Discharge data from Aug 7-8 Storm event



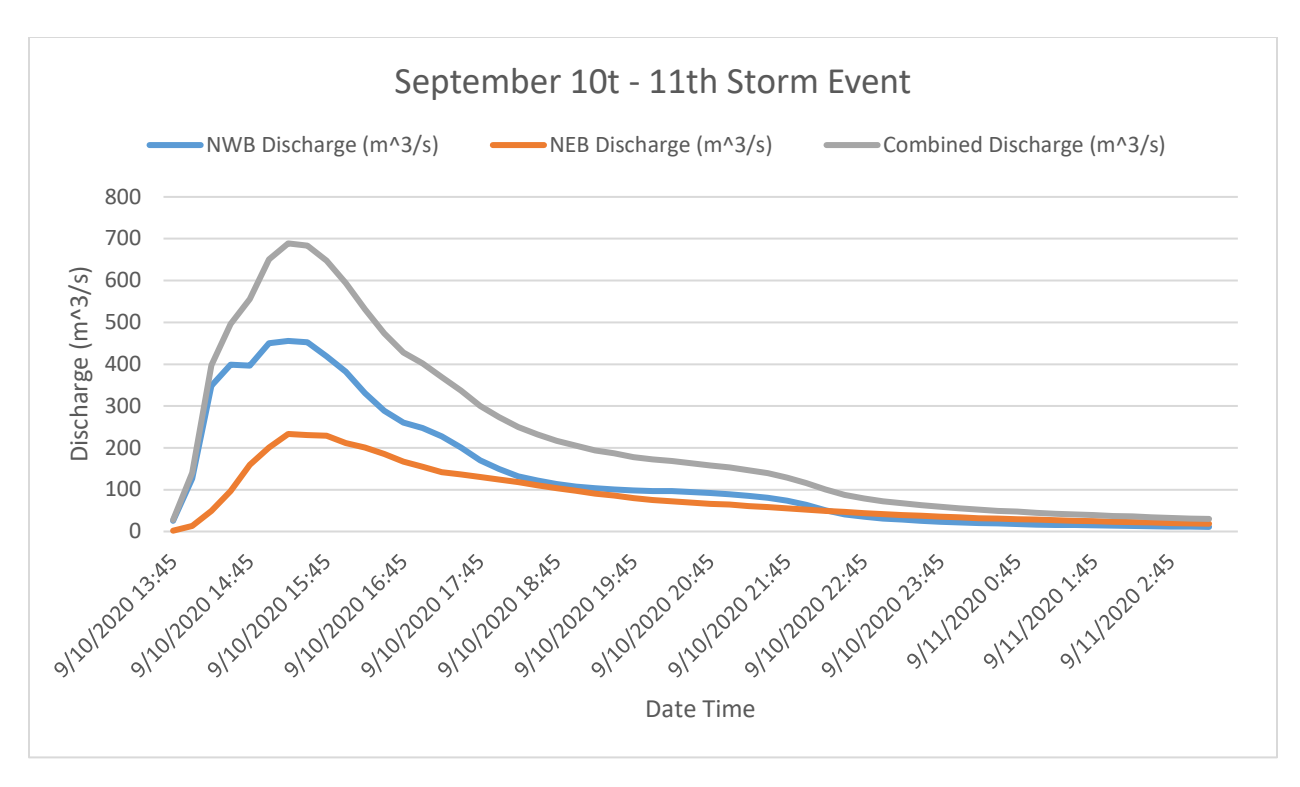
Supplemental 21: Discharge data of August 12-132020 storm event



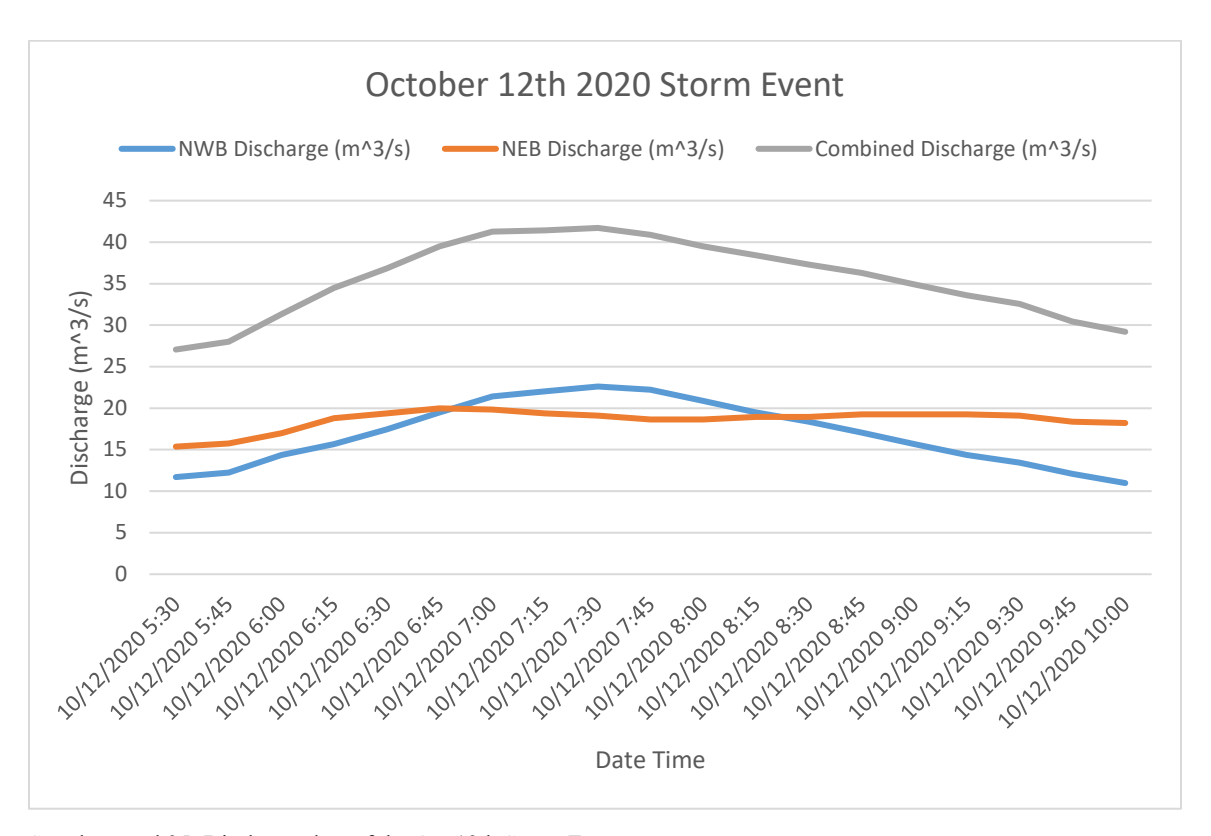
Supplemental 22: Discharge data of August 16 2020 Storm event



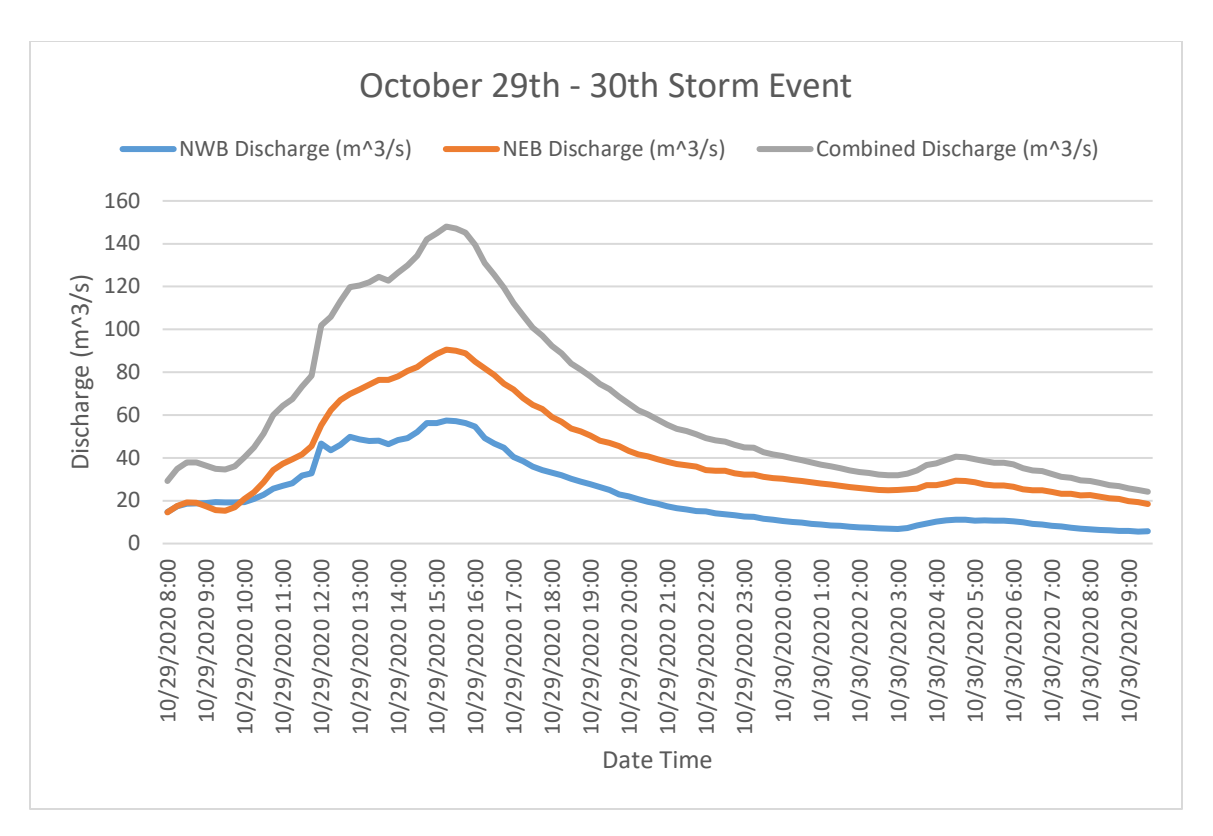
Supplemental 23: Discharge date of Sept 3-4 2020 Storm Event



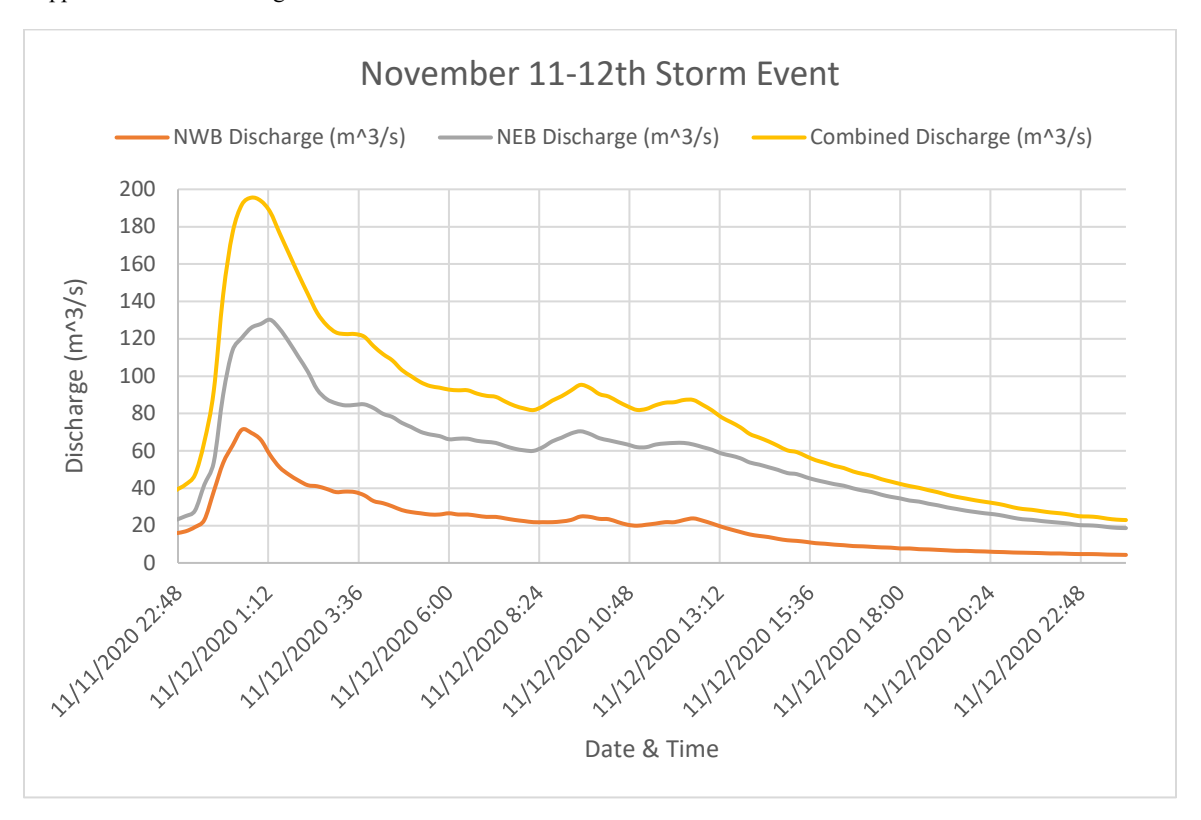
Supplemental 24: September 10th - 11th Discharge Data



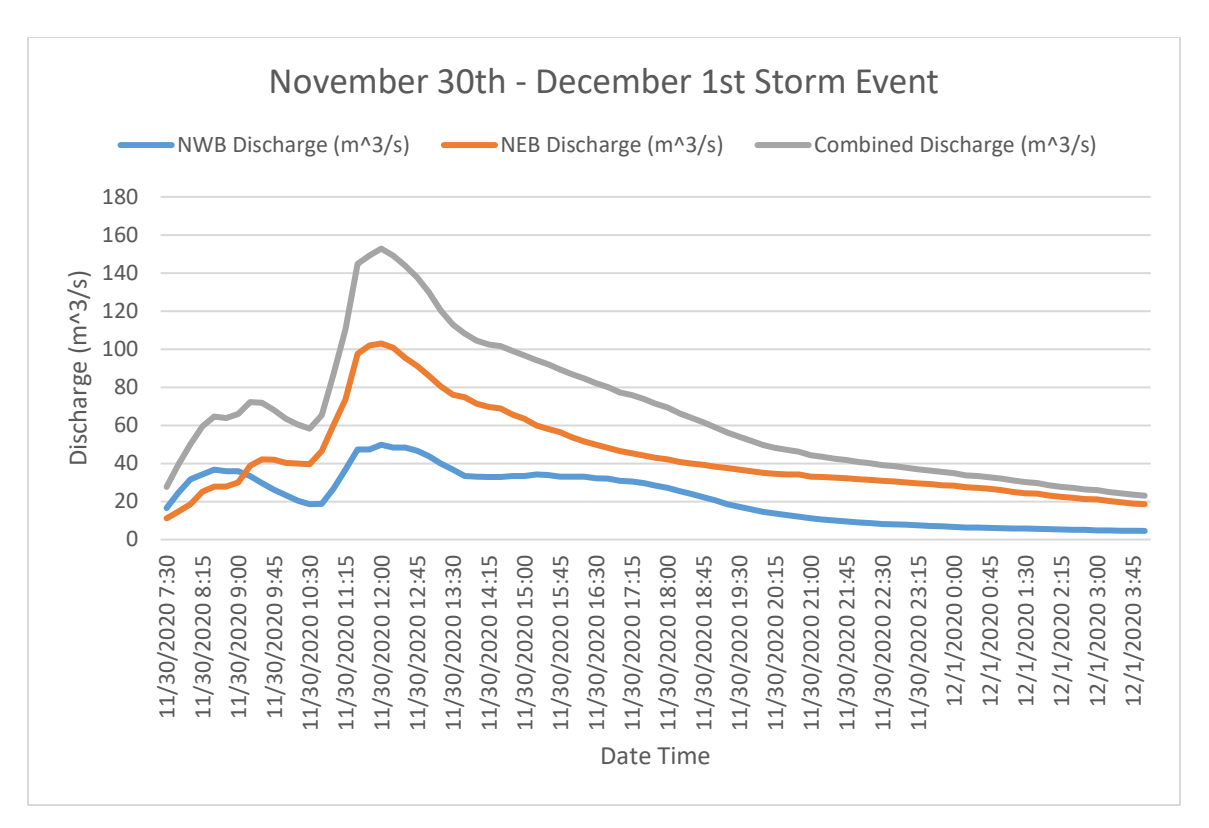
Supplemental 25: Discharge data of the Oct 12th Storm Event



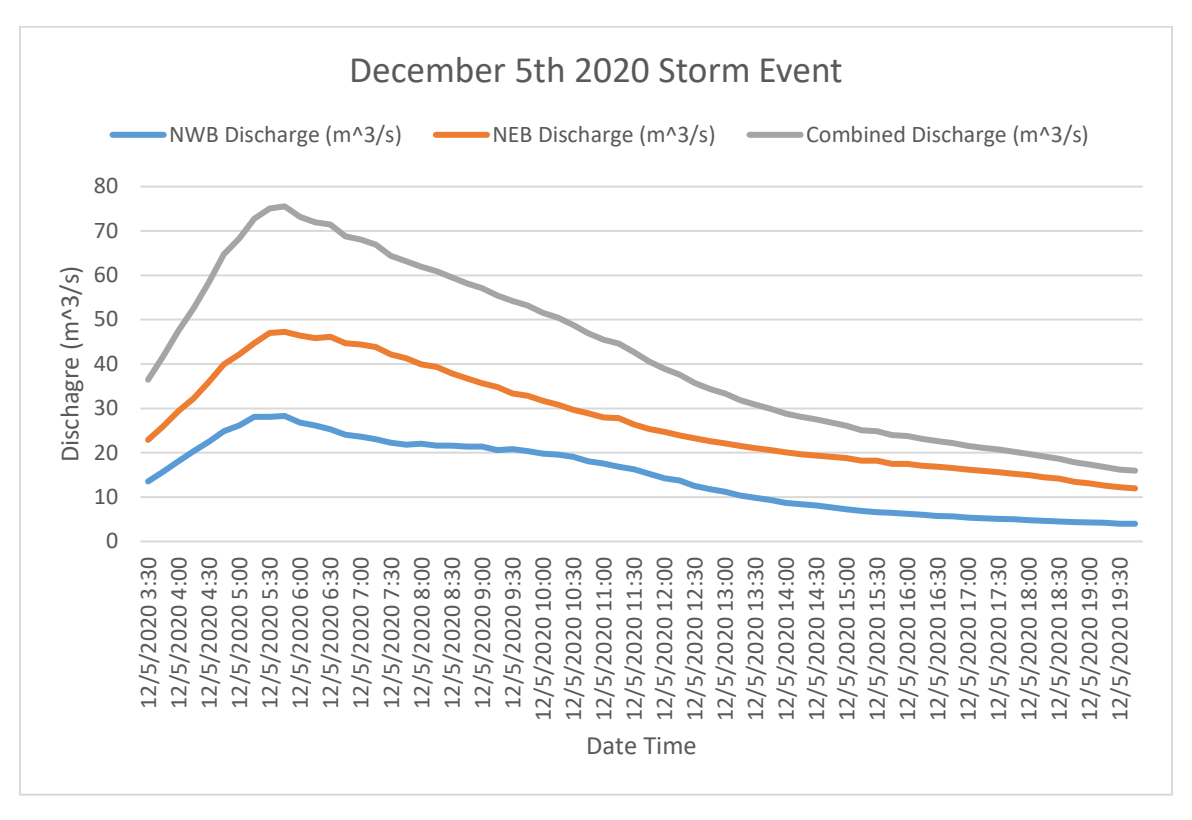
Supplemental 26: Discharge Data of the Oct 29-30 2020 Storm Event



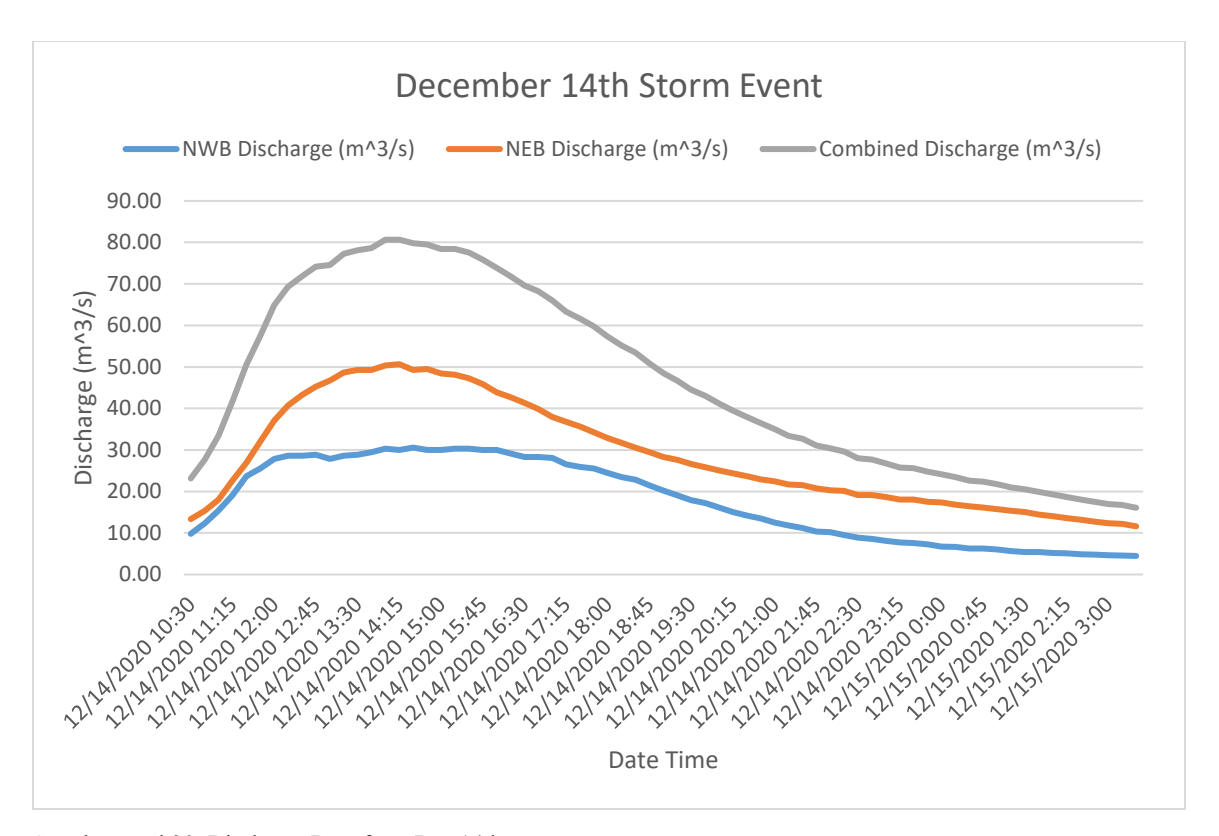
Supplemental 27: Discharge Data from the Nov 11th - 12th Storm Event



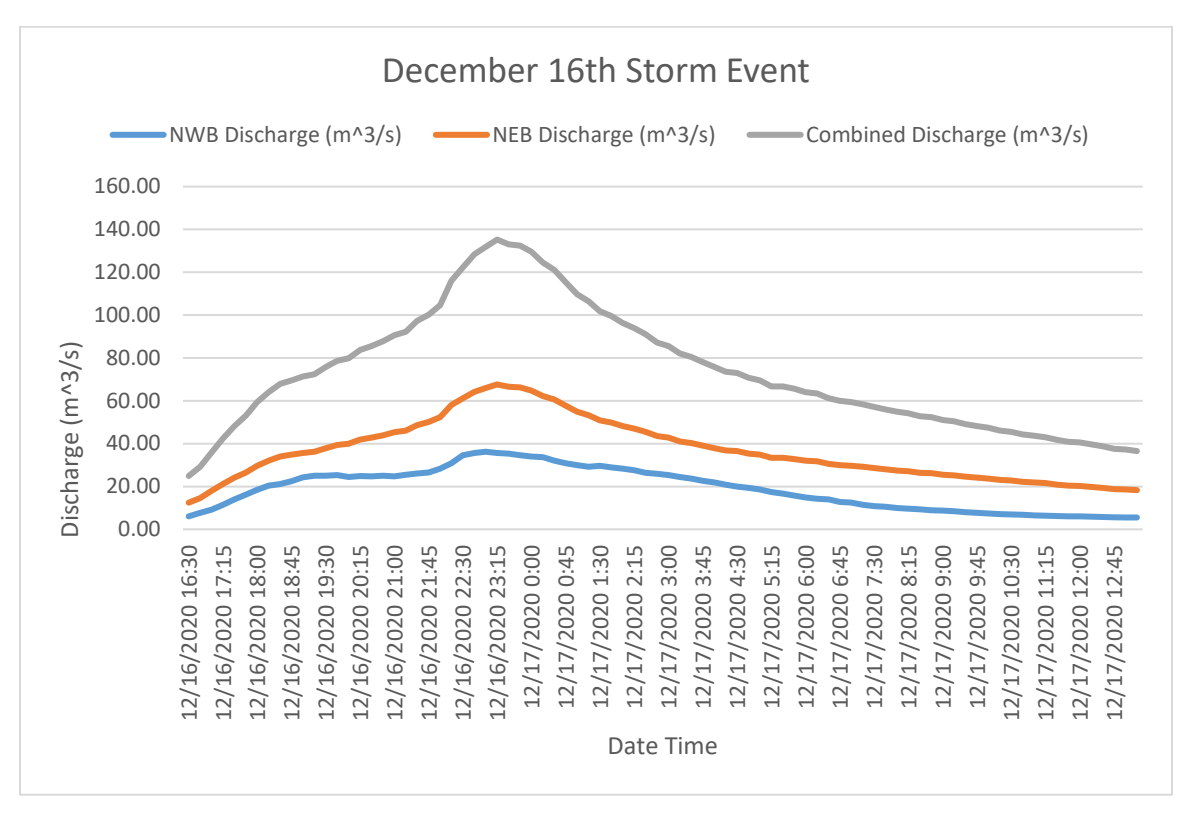
Supplemental 28: Discharge data from Nov 30 - Dec 1 storm event



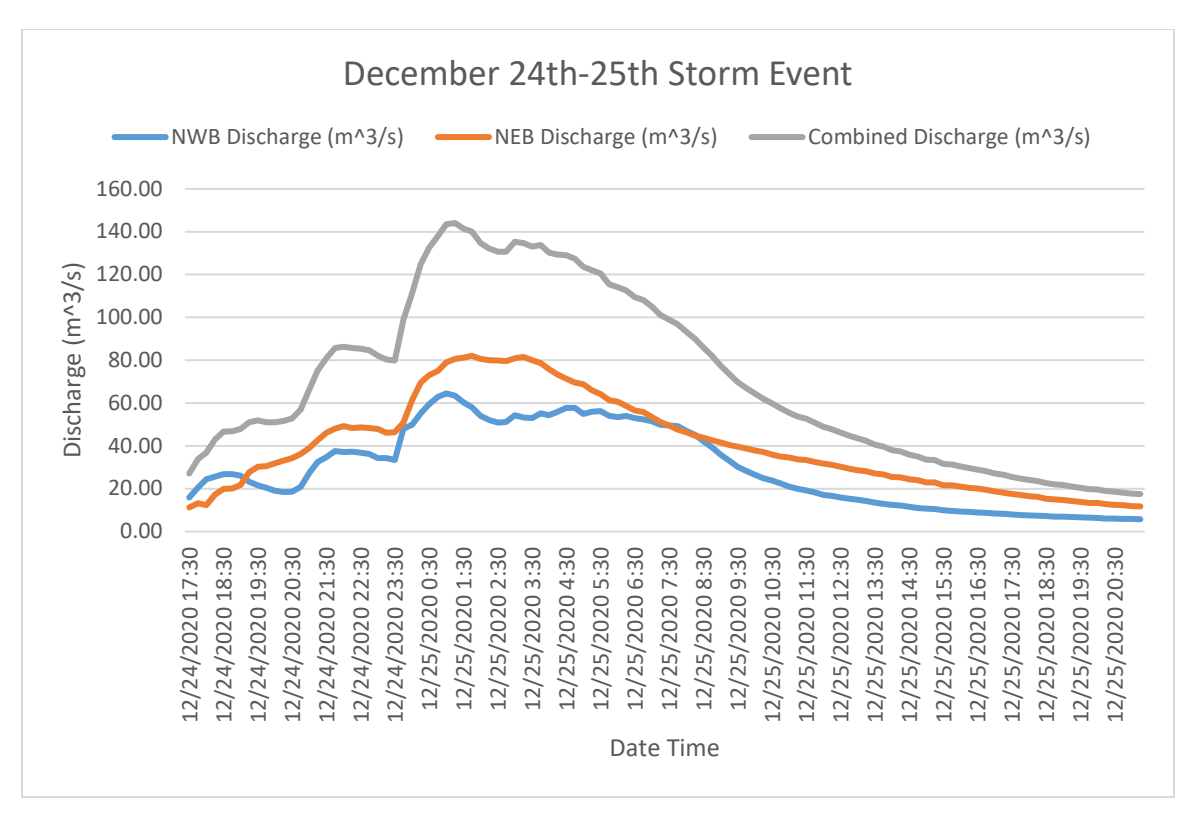
Supplemental 29: Discharge Data from Dec 5th storm event



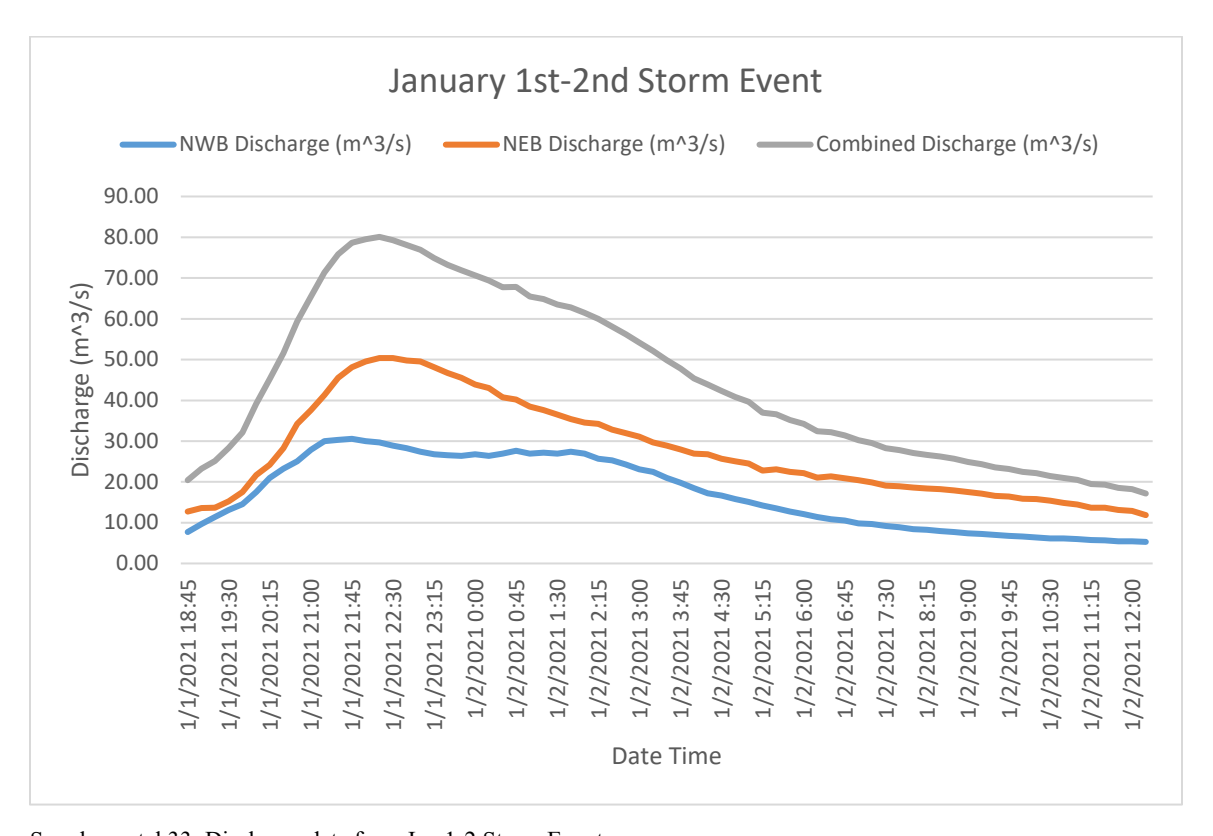
Supplemental 30: Discharge Data from Dec 14th storm event



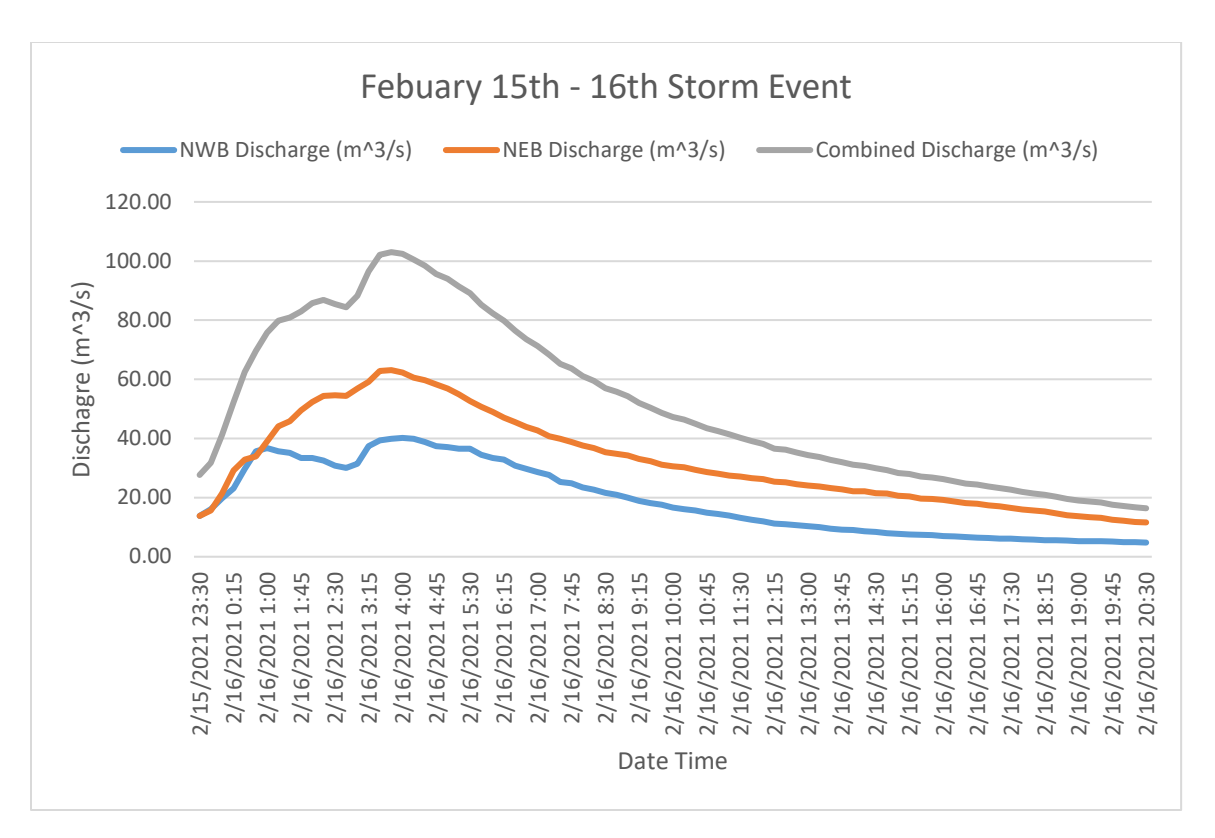
Supplemental 31: Discharge Data from December 16th storm event



Supplemental 32: Discharge data from the Dec 24-25 Storm Event



Supplemental 33: Discharge data from Jan 1-2 Storm Event



Supplemental 34: Discharge data from Feb 15-16 Storm Event